GUIDE BOOK OF
RINJANI CALDERA
POST-CONFERENCE FIELD TRIP

SEPTEMBER 14 - 19, 2014

Tour Leaders:

J.C. KOMOROWSSKY
M. NUGRAHA KARTADINATA
HERYADI RACHMAT
YUDHI WAHYUDI

YOGYAKARTA
INDONESIA

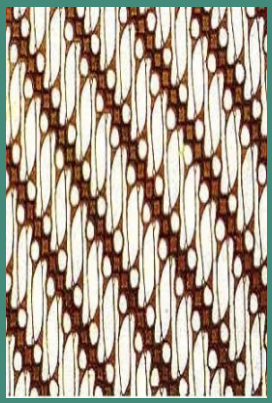

CITIES ON VOLCANOES 8

LIVING IN HARMONY WITH VOLCANO:
BRIDGING THE WILL OF NATURE TO SOCIETY

SEPTEMBER
9 - 13, 2014

GUIDE BOOK OF RINJANI CALDERA
POST-CONFERENCE FIELD TRIP

SEPTEMBER 14 - 19, 2014

Tour Leaders:

J.C. KOMOROWSSKY
M. NUGRAHA KARTADINATA
HERYADI RACHMAT
YUDHI WAHYUDI

CITIES ON VOLCANOES 8

LIVING IN HARMONY WITH VOLCANO:
BRIDGING THE WILL OF NATURE TO SOCIETY

Part 1: General information on the Rinjani volcanic complex and on the AD 1257 eruption, Nusa Tengara Barat Province (island of Lombok), Indonesia

Authors :

M. Nugraha Kartadinata [1], Heryadi Rahmat [2], Yudi Wahyudi [1], Indyo Pratomo [2], Oktory Prambada [1], Jean-Christophe Komorowski [3], Céline Vidal [3], Nicole Métrich [3], Franck Lavigne [4].

1) Center for Volcanology and Geological Hazards Management (CVGHM), Geological Agency, Bandung, Indonesia
2) Geological Museum, Geological Agency, Bandung, Indonesia
3) Institut de Physique du Globe de Paris – CNRS UMR7154, Université Sorbonne Paris-Cité, France
4) Université Paris 1 Panthéon-Sorbonne, Département de Géographie, and Laboratoire de Géographie Physique, CNRS 8591, France

Introduction

Rinjani is the only active volcano in Lombok Island. It is a volcanic complex in which Rinjani is the name of the old active volcano in the area that protrudes as the highest peak in the island of Lombok. Some solfataras and fumaroles still exist in its crater. Apart from Rinjani (3276m asl), there are two other younger volcanic cones (Figs. 11) called Barujari (Tenga, 2376m asl) and Mas (Rombongan, 2110m asl). Between these two young cones, Barujari is the most active where the activity has taken occurred as recently as in 2010. These two young cones are located inside the caldera that contain a large beautiful lake called Segara Anak (1998m asl) (Figs. 13B, 30).

The Segara Anak Caldera Lake is about 11 million m^2, 230m deep with a volume of about 1,375 million m^3. The excess of the lake water flows through Kokok Putih (kokok means river) to the northeastern flank of the caldera (Kusumadinata, 1979).

The latest study revealead that caldera forming eruption occured in 1257 AD creating the formation of caldera so-called Segara Anak caldera (Lavigne et al., 2012; 2013) The caldera forming eruption

produced large scale pyroclastic flows (ignimbrite) consisting dominantly of pumice. These pyroclastic flow deposits almost cover the whole area of the volcano.

During historical time there have been 15 recorded eruptions from Barujari/Rombongan cones since 1847, of which the latest one occurred in May 2010. Although it is not as big as the prehistoric activity, the latest major eruption that occurred in 1994 had indirectly caused the death of several people and property loss as a result of a mudflow (lahar.) DIndeed, during the rainy season, lahar caused 31 people were killed, 4 people were missing, 7 people were injured along Tanggik river. Many hectares of arable land and infrastructures were devastated by the ahar flood.

The beautiful panorama of the Rinjani volcanic complex with its caldera lake and the young active cones inside the caldera has become one of the most popular tourist attractions of Lombok. Its nature, culture, arts and traditional handy crafts constitute exclusive assests that have also contributed to making Lombok an increasingly popular tourist venue. Furthermore, Lombok Island that is located not far from Bali is easily accessible. In addition, to the east of Lombok, across the Alas strait, the beautiful island of Sumbawa also offers great natural and cultural assets for tourism including the famous caldera of Tambora formed in the great explosive eruption of AD 1815.

Aim

The aim of this excursion is to introduce Conference participants to the unique and impressive volcanology of Rinjani Volcano. We hope this will foster an interest among participants to exchange their experiences and develop collaborative research on Rinjani volcano and its related aspects that will expand the scientific knowleddge on this active volcano .

Location

Rinjani volcano is located in the northern tip of East Lombok, whereas Newmont Nusa Tenggara gold and copper mining is located in southwestern part of Sumbawa Island. However, both islands are the main islands of West Nusa Tenggara Province.

These two islands are located east of Bali beyond the Lombok and Alas straits respectively (**Fig. 1**).

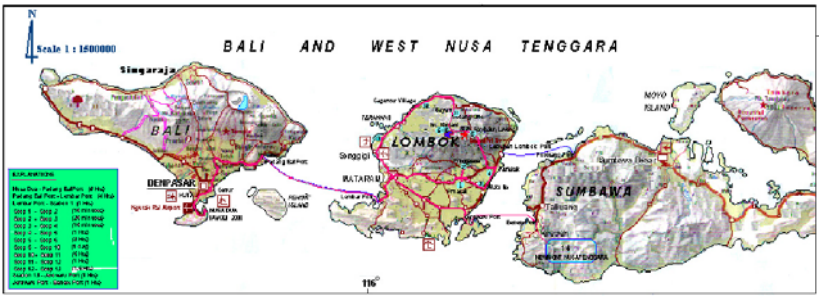

Fig. 1. Field Trip Location Map.

Geological Aspect

Tectonics

According to van Bemmelen (1949) the older basement of Solo Zone in the form of the geoanticline of East Java reappears in western North Lombok, and this pattern of Java seems to end in Lombok. The development of tectonic activity of Lombok was the result of a tectonic uplift, volcanism and intrusive activity (Andi, M et.al, 1992 in Santosa & Sinulingga, 1994).

It is inferred that the oldest tectonic activity in Lombok took place during Oligocene, and that it was followed by submarine volcanic activity of basaltic andesite composition, that resulted in the formation of the volcanic sedimentary rocks of the Pengulung Formation and Kawangan Formation. These two formations are interfingered. This activity took place until Early Miocene and then during Middle Miocene, a post-magmatic activity developped in the form of a dacitic intrusion that intruded the Pengulung and Kawangan Formations.

According to Andrew et.al (1971) in Santosa and Sinulingga (1994), in general, volcanism that developped from the Pliocene until the Recent period along the island arc produced thick sequences of volcanic rocks. He suggests that many eruption centers are associated with a lineament and were controlled by fracture zones or faults that cut across the island arc.

The major elements chemical composition of Rinjani volcanic rocks plots on Pearce diagram (Pearce et.al, 1977) in the geodynamic field of orogenic belts (**Fig. 2**).

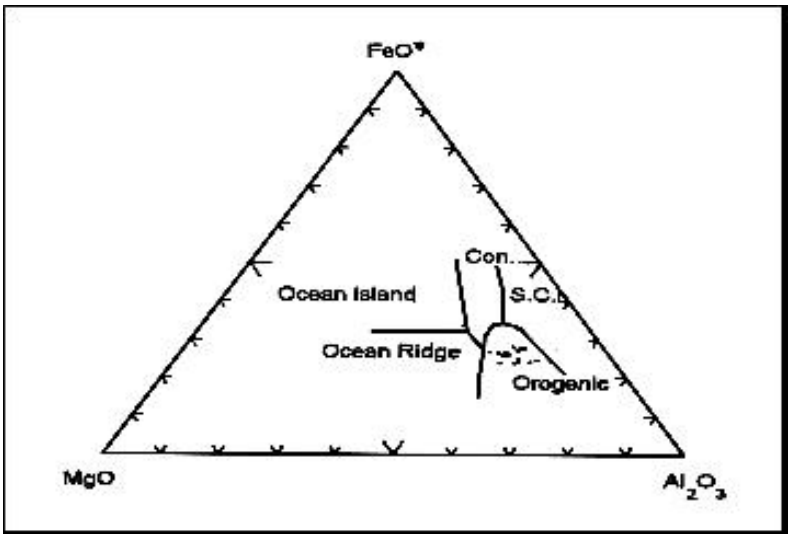

Fig. 2. Tectonic environment of Rinjani volcanic rocks.

During Early Quaternary the tectonic activity in Lombok had caused strike-slip and normal faults.

Physiography

According to van Bemmelen (1949), the northern part of Lombok Island is the continuation of Solo Zone of Java Island. Solo Zone represents the former top part of geoanticlinal belt, which separated from the south flank of the belt (represented by the Southern Mountains) and slipped northward. In the top part of the geoanticline granodioritic plutonic rocks were emplaced during the intra Miocene phase of diastrophism. The basic roof part of such an intrusion is exposed on Java in the Jiwo Hills (west of Surakarta, Central Java), but farther eastward this older basement of the Solo Zone is not exposed anywhere. It appears in western North Lombok, where also the basic roof part of a plutonic intrusion is exposed.

The structural pattern of Java seems to end in Lombok. Farther eastward the geoanticlinal top part has not yet collapsed. In Sumbawa there has been limite gravitational slidding of parts of the North flank occurred.

Blown, in Nasution et.al (1984) proposed that at the end of Tertiary the regional faults of Lombok, with an orientation SW-SE, SSW-NNE and N-S, remained active until Quaternary (**Fig. 3**).

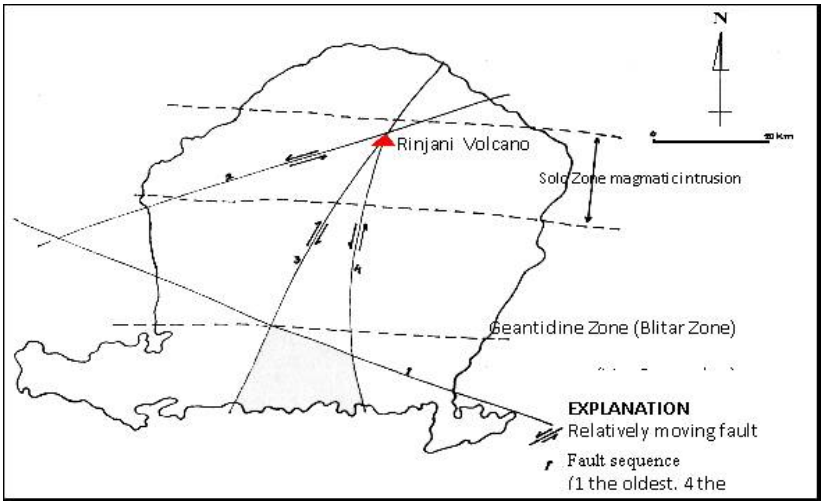

Fig. 3. The regional fault structures of Lombok at the end of Tertiary or early Quaternary by Blown (1974) adapted from Kusnadi & Ilyas, 1997.

Geomorphology

According to van Padang (1951) in (Kusumadinata, 1979), Rinjani is a composite volcano protruding high up in the North of Lombok. It is mostly composed of young volcanic rocks. Rinjani cone (3726 m asl) is steepest and highest peak in the area. It consists of mostly of a thick succession of loose tephra fallout layers with a crater on the summit area. A large eliptical caldera (8.2 x 5.4 km) that contains the beautiful Segara Anak Lake is located just to the West of Rinjani **(Fig. 13B; 29; 30**).

The eastern part of Segara Anak Lake is filled with the new active volcanic cones of Barujari/Tenga (2376m asl) and Gunung

Mas/Rombongan (2110m asl) closer to the center of the lake (**Fig. 4; 11, 13B; 29; 30**). Both of these young volcanic cones are composed of lava flows and loose material that resulted from strombolian eruptions.

Fig. 4. Active volcanic cones inside the Anak Segara caldera of Rinjani volcano complex.

The other volcanic cones in the surrounding area are located around or on the rim of the caldera: Mt. Kondo (2914 m asl) on the SW rim, Mt. Sangkareang (2914 m asl) in the NW rim and Mt. Plawangan (2658 m asl) in the NNE rim of the caldera. About 12 km northeast of Rinjani the plateau of Sembalun Lawang is located at an elevation of 1000 m above sea level.

The southern flank of Rinjani is more perfectly developed than the northern, eastern and western flanks, where other old volcanic edifices have limited the development of Rinjani.

Stratigraphy

On the basis of Mt. Rinjani Geological Map (**Fig. 5**), the stratigraphy of Rinjani volcanic complex can be divided into units of eruption products that consists of several eruptive vents, namely: Old Rinjani, Mt. Kondo, Mt. Sangkareang, Mt. Rinjani, Mt. Barujari, Mt. Mas and Mt. Manuk. Some of them such as Old Rinjani, Kondo and Sangkareang cannot be recognized by their old crater as they have been destroyed as a result of the formation of the caldera.

Nevertheless, there is still abundant geological evidence of the location of former volcanic edifice in the presence of eruption products, dykes, hot spring and alteration zones developped in the host rocks (Hendrasto et.al, 1990).

In general the eruption products are distributed on to the northern and southern flanks, but to the east and western flanks their distribution was limited by the older volcanic edifices of Punikan complex and Anak Dare complex.

The stratigraphic succession was defined based on the basis of lithological contacts and superposition of rock units. But, for those where the contact cannot be observed, the stratigraphy was defined by comparing the types of lithologies, their degree of weathering and erosion. Mapping of volcanic units was achieved base on the analysis of aerial photographs.

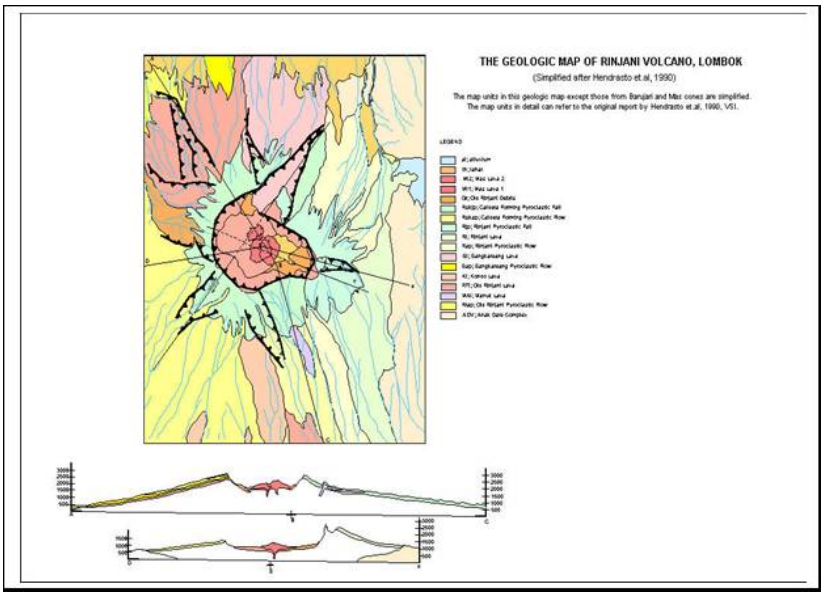

Fig. 5. Geological map of Rinjani volcano (Hendrasto, et. al., 1990)

Based on the above criteria Hendrasto et.al (1990) described the stratigraphy of Rinjani complex from old to young as follows (**Fig. 5**) :

1) The Old Volcanic Complex consists of: a) Buanmangge and Punikan; and b) Anak Dare Complex
2) Pre-caldera products resulted from eruptions of Rinjani, Mt. Kondo, Mt. Sangkareang and Young Rinjani
3) Caldera eruption products of Old Rinjani
4) Post-caldera eruption products of Barujari Cone, Mas/Rombongan Cone and the secondary products that consist of lahar, volcanic debris avalanche and alluvial deposits.

Petrology and Geochemistry

Based on petrographic and chemical analysis of some lava flows of Rinjani caried out by Santosa and Sinulingga (1994), there are some similarities between lava flows of Rinjani and those from Java Island. Generally these lava flows are porphyritic and intergranular in texture with plagioclase, pyroxene and olivine phenocrysts. For those that have intergranular texture, the pyroxene and olivine minerals are frequently found amongst the irregular and elongated plagioclase minerals. Apart from phenocrysts, the plagioclase is also found as groundmass microlites. This plagioclase is also often associated with opaque minerals, pyroxene and glassy groundmass. The crystals are generally subhedral to euhedral shaped. Based on extinction angle of the albite twin and abundant of zoning, they are mostly labradorite.

The pyroxene of Rinjani lava flows are mostly found as phenocrysts (20%), subhedral – euhedral crystals with prismatic shapes. They show simple and polysynthetic twinning, and they vary from ortho pyroxene to clino pyroxene.

The olivine minerals are sub-hedral – anhedral found as phenocrysts in relative small amount that ranges between 1 to 5 %. The olivine minerals are usually found between plagioclase minerals.

The opaque minerals are found almost in all thin sections as the groundmass is anhedral crystals. From the thin sections it is found that the lava flows of Rinjani range between basalt –basaltic andesite.

Chemical analysis of some rock samples of Rinjani volcano shows that the silica content varies from 48.95 % to 56.86 %. The TiO content is less than 1 %, and there are only 2 rock samples that

show 1.02 % and 1.04 %. This is typical of lava flows from island-arcs (Santosa & Sinulingga, 1994).

On a Le Maître diagram of SiO_2 against K_2O, the composition of Rinjani eruption products range from basalt to basaltic andesite (fig.6).

The magmatic evolution during differentiation has resulted in negative correlation between the content of SiO_2 and Na_2O. The existence of decreasing Na_2O content provides evidence for fractionation of pyroxene and plagioclase crystals. The plot of other major elements such as Al_2O3, Fe_2O_3, MgO and CaO show a decreasing trend with respect to SiO_2 (**Fig. 6**).

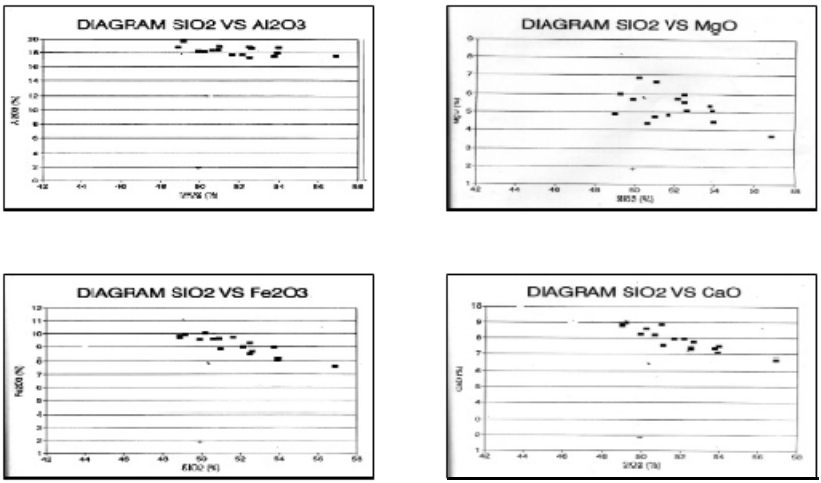

Fig.6. Plot of Al_2O_3, Fe_2O_3, MgO and CaO against SiO_2 showing negative pattern.

This pattern provides evidence for a process of normal fractionation related to the presence of dominant plagioclase, pyroxene and olivine as phenocrysts. These elements are also the main forming elements of the above minerals (Santosa & Sinulingga, 1994).

Geothermal Energy

A geothermal field is found in the area of Sembalun Lawang to the east northeast of Rinjani volcano (**Fig. 7**).

The geothermal manifestation of Sembalun area is characterized by the existence of hot springs and areas with altered volcanic rocks. There are three hot springs in the outer side of Sembalun caldera, whereas the alteration of volcanic rocks is found in the Sembalun lava flow unit, called Aik Orok altered zone. These three hot springs are Aik Kukusan, Aik Kalak and Aik Sebau ;

Fig. 7. Location map of Sembalun geothermal field, Lombok Island.

- Aik Kukusan hot spring is located in Sembalun stream, at 850m asl, T = 44^0C, no sulphuric gas smell, it is controlled by an E –W trend fault.
- Aik Kalak hot spring is located at Sambelia stream, at 950m asl, T= 41^0C, no sulphuric gas smell, it is controlled by a W—E trend fault
- Aik Sebau hot spring is located in the south of Mt. Pusuk, at 1050m asl, T = 34^0C, sulphuric gas smell, it is controlled by a NW—SE trend fault
- Aik Orok altered zone is located in the SE part of the caldera floor, at 1300m asl, it seems that the alteration is also influenced by a NW—SE trend fault

This geothermal field is part of a volcano depression that resulted from caldera formation during the activity of Sembalun volcano pre-historic time to Early Quaternary (Sundhoro, 1992). This large

eruption produced a large volume of andesitic pyroclastic flows associated with andesite—dacite pumice fallout. The volcanic activity history of Sembalun volcano is shown in **Figure 8**.

The collapse of the roof of magma chamber resulted in a caldera structure that formed a ring fractures system. The Sembalun caldera has an elliptical shaped which is 7 x 4 km in size that is facing northwestward.

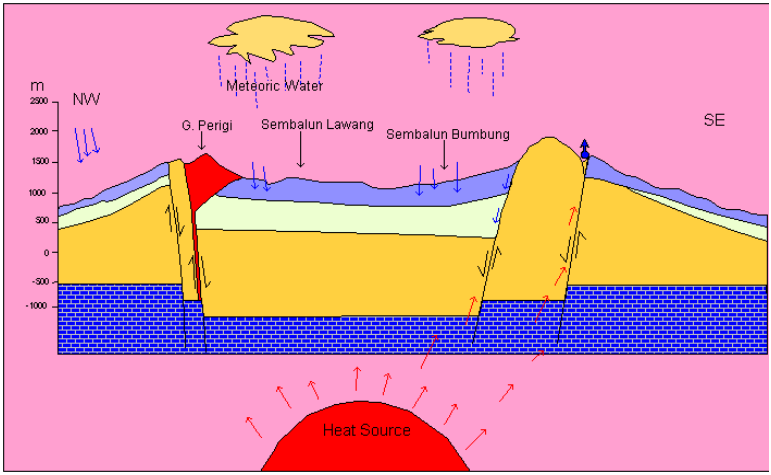

Fig. 8. Volcanic activity history and volcanism model of Sembalun volcano (taken from Sundhoro, 1992).

Geophysical survey (gravity and resistivity) shows that Sembalun depression is a caldera floor (Simanjutak 1988 in Sundhoro, 1992). **Figure 9A** shows vertical section of the resistivity line A, Sembalun geothermal field (Sundhoro, 1992).

Chemistry of three hot springs found in the area shows that they can be divided into two systems, namely :

- Acid sulphate rich water system (Aik Kalak and Aik Kukusan hot springs) and
- Chloride sulphate rich water system (Air Sebau hot spring)

The acid sulphate rich water contains high SiO_4 and relatively small HCO_3^- and Cl^-. This suggests that the reservoir for Aik Kalak and Aik

Kukusan hot springs is a steam system (Sundhoro, 1992). Survey and modelling by Nasution et al. (2010) in the Propok-Sembalun area show the existence, at depth, of several resistivity layers and fluid flow from depth (**Fig. 9B**). Nasution et al. (2010) interpret this data as representing possibly the existence of a geothermal reservoir at depths of 1500 to 3000 m below the Propok-Sembalun buried caldera systems. A dioritic basement pluton at depths of 3000 to 6000 m is evidenced as a source of deep heat.

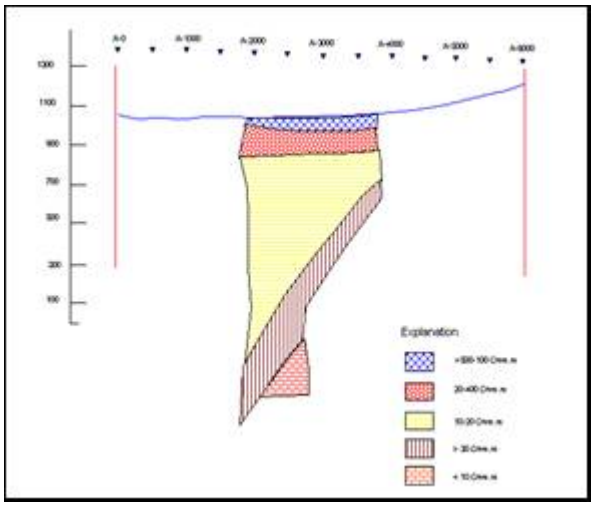

Fig.9.A Vertical section of the real resistivity of line A (Sundhoro, 1992).

The chloride sulphate rich water contains high Cl^- and $So4^=$ and relatively small HCO_3^-. This suggests that the reservoir of Aik Sebau hot spring is a hot water system (Sundhoro, 1992).

Volcano Tourism

Rinjani was selected to become a National Park given its outstanding natural resources. The thick rain forest and the surrounding volcanic areas have made Rinjani a unique and fascinating place to visite for domestic as well as international tourists.

Indeed, the remote volcanic scenery of Rinjani volcano, Segara Anak Caldera Lake and the two young active cones constitute a landscape of exceptional beauty and diversity where unique fauna and flora can also be observed. The aim of Rinjani National Park is to preserve these natural wonders for Indonesia as well as for scientific studies.

For those who are interested in mountain climbing and hiking, camping and even fishing Rinjani is a good place to visit. Some hot springs are also found either around Segara Anak Caldera area or in the lower flank like in Sembalun Lawang to the northeast of Rinjani

Nice waterfalls and fresh water springs are quite common around the volcano and often used by people for drinking and other purposes during climbing to the summit or for recreational purposes.

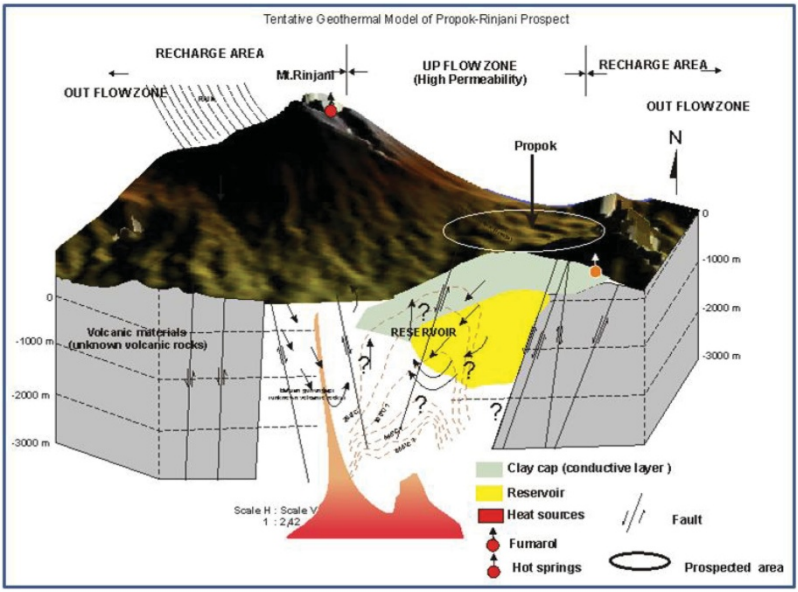

Fig.9B. Geothermal tentative model of the Propok-Rinjani geothermal system (taken from Nasution et al., 2010).

To support this volcano tourism, the Local Government in cooperation with private foundations and the Department of Forestry has been developing facilities throughout the Rinjani National Park to

meet the requirements and standards of a National Park, namely footpaths, public toilets, camping ground etc.

Volcano Monitoring

Compared to Merapi, Semeru or Karangetang volcanoes, Rinjani is not classified as a very active volcano. Therefore, this volcano is monitored with a standard monitoring system except during eruptions or an increase activity.

Rinjani volcano is monitored visually and seismically from the Volcano Observatory at Sembalun Lawang village (1000 m asl) that is located to the northeastern part of the volcano **(Fig. 10A**).

Fig. 10A. The Volcano Observatoy of Rinjani at Sembalun Lawang.

Visual observation is continually carried out by the observers from the Observatory. Monitoring comprise measurements of temperature, weather and seismicity periodically, as well as the measurement of the temperature of the crater of Barujari cone, hot springs and lake water around Segara Anak Caldera. However given the rugged topography, the difficult conditions, and the great walking distances involved, these temperature measurements are undertaken only periodically.

Rinjani/Barujari volcano, which is located some 12 km to the northeastwards of the Observatory is only equipped with one component Seismograph of PS-2 type (wire system). Data analysis of seismicity is carried out by using statistical method. The result of the seismic observation such as the amount of earthquakes and its parameter are plotted in a graph against time.

As evidenced from its shape, the nature of its current activity and its position inside the caldera of the AD 1257 eruption, the new volcanic cone of Barujari is quite young. The products of this new cone consist of lava flows and loose ejected pyroclastic material. The composition ranges from basalt to basaltic andesite, therefore, the magnitude and intensity of the eruptions have remained low (Santosa & Sinulingga, 1994).

Since 1847 there have been 15 eruptions during historic time (Table 1), with the latest eruption occurring in 2010 (Kusnadi et.al, 1994; CVGHM; Global Volcanism Program). Sulaeman and Muarif (1998) also suggest that the eruption of Rinjani in 1994 was preceded by phreatic activity, followed by the extrusion of lava flows and tephra emission (**Fig. 10B-C**).

On the basis of confirmed eruptions (Table 1), the shortest repose period of Barujari eruptions is 1 year and the longest is 37 years. This means that eruptions can occur any time. But, from the record of historic eruptions, we know that they did not cause many victims or severe devastation, except an eruption in 1994 where 31 people killed, 4 people missing and 7 people injured and hectares of arable land was devastated by its lahar on the 3rd of November 1994 (CVGHM; Global Volcanism Program).

An eruption began at Barujari on 1 October 2004 and consisted in continued explosions that produced ash columns that reached 300 to 800 m and caused gray thick ash columns to drift N (CVGHM; Global Volcanism Program).

In May 2009 a new eruption began that was accompanied by significant volcanic seismicity. Eruptive activity which was visible from Sembalun Lawang, 15 km East, consisted of the continuous ejection of glowing material that reached 200 m in height above the vent, and was thrown laterally out to a radius of 500 m from the summit. A great amount of ash, cinders, and incandescent material

fell into the caldera, while smaller fragments were blown away. By August 31 the eruption was still underway and a large lava flow (Fig. 11) had covered an area of 0.65 km^2. The lava entered Segara Anak Lake and significantly modified its shoreline and reduced its surface area by 0.46 km^2.

During May 2010, eruptions of Barujari ejected incandescent material and ash that reached an altitude of 5.5 km. Drifting ash plumes caused significant damage 12 km downwind. Lava flowed into the lake and caused its temperature to rise from 21 to 35 °C (CVGHM; Global Volcanism Program). The eruption products from these recent eruptions (lava flows, **Fig. 11**) and large incandescent blocks are confined to Segara Anak caldera, except the finer grained tephra that were dispersed farther in the surrounding areas.

Fig. 10B. Eruption of Barujari in 1995. (Image Oliver Spalt/Wikimedia, http://7img.com/i/Rinjani_1994_gedDKbqz).

Fig.10C. Explosion from Barujari cone at Rinjani volcano on June 9, 1994 and emplacement of a small pyroclastic flow (Photo CVGHM; Global Volcanism Program).

Fig. 11. 3D satellite view of Barujari cone on 26 June 2012 and recent lava flows. Geoeye-1 Satellite Image © Centre for Remote Imaging, Sensing and Processing, National University of Singapore (2012), terrain views rendered using SRTM 3 data from NASA.

Hazard Zone

Historical Eruption

The Volcanic Hazards Map of Rinjani Volcano (**Fig. 12**) has been made by Hadisantono et al. (2008). This map is provided to anticipate the hazard of Rinjani volcano in the case of any renewed activity in the future. This map is used as tool to assist the mitigation of volcanic risks for the people living around the volcano as well as inform them on appropriate evacuation routes. The volcanic hazard map also describes the kind and types of volcanic hazard expected. It was compiled based on the morphology, past eruption history and distribution of eruption products.

Table 1. Recorded eruptions of Barujari (Rinjani volcanic complex) since 1847 (CVGHM; Rinjani Observatory, CVGHM; Global Volcanism Program)

Year of eruption	Rest period (in years)	Estimated erupted lava flow volume in million m^3
1847	?	
1884	37	
1900	16	
1901	1	
1906	5	
1909	3	
1915	6	
1944	29	73.3
1949	5	
1953	4	
1966	13	6.6
1994-95	28	25.4
2004	10	
2009	5	?
2010	1	

The Samalas AD 1257 eruption

Although they are very low-frequency events, caldera-forming volcanic eruptions can discharge in the atmosphere tens to thousands of km^3 of finely fragmented magma and large amounts of associated sulfur and halogen gasses on timescales of a few hours to days. In the past, such high-impact events have had devastating consequences both locally and on a global scale (Miller and Wark, 2008). Caldera-forming eruptions of that scale have never been observed nor monitored. Hence, the precursory signals associated with production and ascent of large magma volumes are not well understood. The global environmental impact of caldera eruptions also must be better constrained. High-resolution physical

volcanological data on erupted products and geochemistry of associated volatiles are needed to better reconstruct past events, understand their causal processes and produce calibrating data for computer modeling of global environmental change and impact due to volcanic forcing.

In recent years the potential impact of volcanic eruptions on global climate has been the subject of intense research with major implications (e.g. Miller et al., 2012; Schneider et al., 2009, Sigl et al., 2014). Many researchers have linked ecological, environmental and historical phenomena to the occurrence in a tropical setting of a large-scale 13th century mystery eruption responsible for the largest concentration of volcanic sulfate in ice cores in the last 7000 years (Palais et al., 1990; Zielinski et al., 1994) that thus likely had a global impact including the great mid-13th century stratospheric dust veil (Oppenheimer, 2003; Stothers, 2000). El Chichon (Mexico) and Quilotoa (Ecuador) volcanoes were proposed as potential candidates for this mystery eruption that was hypothesized to have erupted a volume much larger than the largest recognized historic eruption of Tambora volcano in 1815 (Indonesia) that produced ca. 50 km^3 of magma (Sigurdson and Carey, 1989; Self et al., 1984; 2004).

Polar ice core records attest to a colossal volcanic eruption that took place ca. A.D. 1257 or 1258, most probably in the tropics. Estimates based on sulfate deposition in these records suggested that it yielded, ca. ≥ 100 Tg of sulfur (Oppenhiemer, 2003; Oppenheimer et al., 2011; **Fig. 13A**) corresponding to the largest volcanic sulfur release to the stratosphere of the past 7,000 years (Palais et al., 1990; Zielinski et al., 1994; Gao et al., 2007;), more than twice that of the AD 1815 Tambora eruption.

These figures have been revised with additionnal and more robust data from the comprehensive new analysis of a much larger ice core database of Sigl et al. (2014) who confirm that the AD 1257 eruption of Samalas produced the largest sulfate spike in Antarctic ice cores over the last 2000 years and out of the 30 largest documented eruptions.

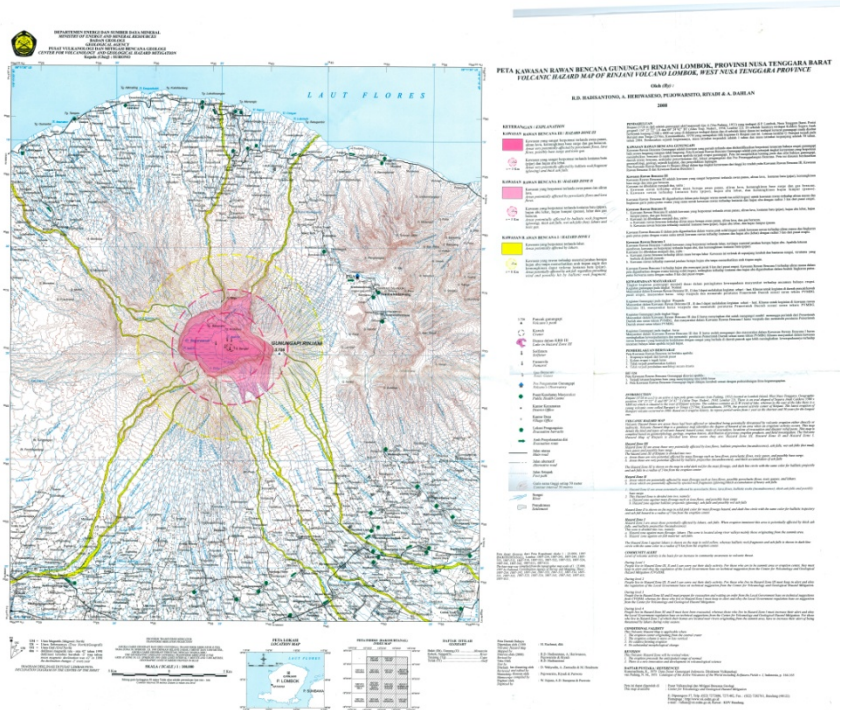

Fig. 12. Volcanic Hazard Map of Rinjani Volcano (Hadisantono, et.al, 2008)

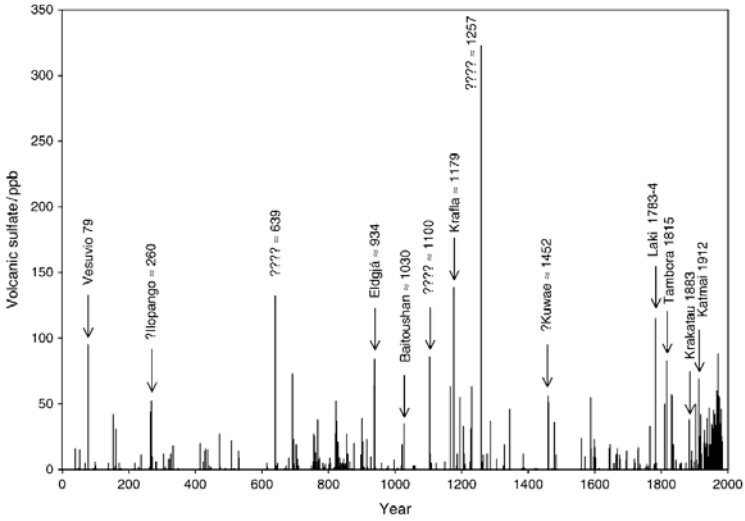

Fig. 13A. Volcanic sulphate record in the GISP2 Greenland ice core and potential source volcanic eruptions of the last 2000 years (taken from Oppenheimer, 2003).

Furthermore, although they reduce by 15% the sulfate contribution of the AD1257 Samalas eruption compared to data published by Gao et al. (2008), the best results from the modelling of the sulfur stratospheric load necessary to produced the observed sulfate spikes in Antarctic ice cores suggest that Samalas might ejected 170 Mt of SO_2 in the stratosphere compare to 45 Mt of SO_2 for the 1D 1815 Tambora eruption (Sigl et al., 2014). Tree rings, exegesis of local and European medieval historical chronicles, and computational models corroborate the expected worldwide atmospheric and climatic effects of this eruption (Lavigne et al., 2013). However, until now there has been no convincing candidate for the mid-13th century "mystery eruption." Identification of the volcano responsible for the mid-13th century mystery eruption has eluded glaciologists, volcanologists, and climatologists for three decades. Takada et al. (2003) and Nasution et al. (2004), had suggested that the caldera-forming eruption of Rinjani had occurred in the 13th century based on radiocarbon dates on charcoal and field data. On the basis of extensive new field data on tephra dispersion

and stratigraphy, preliminary eruptive dynamics data, new radiocarbon age dates, as well as the exegesis of local and European medieval historical chronicles evidence, Lavigne et al. (2012;2013) identified the Rinjani volcanic complex as the source of this major explosive eruption. In addition, the correlation in glass geochemistry of the associated pumice deposits with that of shards found in both Arctic and Antarctic ice cores (Lavigne et al., 2012; 2013), the tropical location of the volcano, and the size of its caldera provide (**Fig. 13B**) compelling evidence to link the prominent A.D. 1258/1259 ice core sulfate spike, and the likely global impact it implies (Oppenheimer, 2003; Stothers, 2000) to the eruption of Samalas (Lavigne et al., 2012; 2013). Moreover, tephra dispersal patterns based on tephra dispersal and historical records, suggested to these authors that it occurred between May and October A.D. 1257.

Analysis of the Babad Lombok, an historical poem written in Old Javanese on palm leaves (Wacana, 1979), allowed Lavigne et al. (2013) to identify an older stratovolcano, Samalas, as the edifice whose top was removed by the caldera-forming eruption of AD 1257:

> *« 274. Mount Rinjani avalanched and Mount Salamas collapsed, followed by large flows of debris accompanied by the noise coming from boulders. These flows destroyed (the seat of the kingdom) Pamatan. All houses were destroyed and swept away, floating on the sea, and many people died.*
>
> *275. During seven days, big earthquakes shook the Earth, stranded in Leneng (Lenek), dragged by the boulder flows, People escaped and some of them climbed the hills.*
> *276. Hiding in Jeringo (close to Mataram), all people moved with the rest of the king's family to several places: Samulia, Borok, Bandar, Pepumba Pasalun, Serowok, Piling, and Ranggi, Sembalun, Pajang, and Sapit.*
>
> *277. At Nangan and Palemaron, big boulders rolled with soil, with pumices and sand, and granite sediments on the land, they evacuated to Brang Batun.*
>
> *278. There were people moving to Pundung, Buak, Bakang, Tana Bea, Lembuak, Bebidas, some of them evacuated to*

Kembang Bumi, Kek- rang, Pengadangan and Puka Puka hate-hate lungguh and also to Langko and Pejanggik.

279. Everybody took refuge together with the King, Lombok became very quiet, even seven days after the earthquakes occurred, and later they built their own houses.

Fig. 13B. Space Shuttle image of Segara Anak caldera (white triangle Plawangan camp site), Rinjani Volcanic Complex, 2002, ISS005-E-15296.jpg (NASA; Global Volcanism Program).

Based on additional extensive fieldwork and laboratory data work, in a new study, Vidal et al. (2013; 2014; in prep.) propose a significantly refined and revised stratigraphy including the identification of several phreatoplinian fallout units, very distal mobile turbulent dilute pyroclastic density currents, voluminous ultraplinian distal fallout units (**Figs. 14, 15, 16**). This provided an opportunity to test new data processing protocoles (e.g. Bonadonna & Costa, 2013) to quantity eruptive dynamics for this large caldera-forming ultraplinian

eruption that produced at least 40 km^3 (dense-rock equivalent) of juvenile material. This complex multiphase eruption involved (**Figs. 14, 15, 16)**: (i) an initial ultraplinian phase UP1 that produced a widespread pumice fallout (7.2 km^3 bulk) from a 36-38 km-high stable column with a mass discharge rate of 1.9-2.6x10^8 kg/s over 5-9 hours (**Fig. 17A)**; (ii) a phreatoplinian phase PP that produced widespread distal mobile and dilute turbulent pyroclastic flows that reached 25-50 km distance and 1.5-2.4 km^3 (bulk) of thick accretionary lapilli-rich fine ash and associated pumice fallout (**Fig. 17B**); and (iii) a second ultraplinian phase UP2 that produced a 17.7 km^3 (bulk) pumice fallout (**Fig. 17C)** from an unstable column that culminated at a height of 41-44 km with a peak mass eruption rate of 3.6-5x10^8 kg/s over 4-6 hours. Based on stratigraphy, sedimentology, and trace elements geochemistry we identified UP2 distal deposits 380 km from source in a lake core studied by Rodysill et al. (2012). UP2 climaxed with the formation of a 6.5x8 km wide caldera (**Fig. 13**) and wholesale column collapse that produced voluminous (ca. 8 km^3 inland bulk, Lavigne et al., 2013) non-welded pumice-rich pyroclastic density currents that entered the sea 25-30 km from source producing an extensive co-PDC ashfall deposit. With a magnitude of 7 and an intensity of 12, the AD 1257 eruption thus ranks among the largest explosive and few ultraplinian eruptions of the Holocene.

Whole-rock analysis of juvenile pumices from plinian fallout units indicates a range of trachytic magma batches (63-65 wt% SiO_2). These magmas share Nb/Th (0.9) and Nb/Zr (0.04) ratios with a pre AD1257 high alumina basaltic magma (Vidal et al., 2013), suggesting that they belong to the Rinjani calc-alkaline suite (Foden, 1983). Extensive laboratory analysis of the volatile content and modelling of magma degassing during this eruption is presently underway.

The identification of this exceptional eruption of Mount Rinjani-Samalas places another Indonesian volcano (along with Toba, Tambora, and Krakatau) in the spotlight of efforts to understand the abrupt environmental and societal changes associated with major episodes of volcanism and caldera genesis (Stothers, 2000). Archaeologists recently determined a date of A.D. 1258 for mass burial of thousands of medieval skeletons in London (Connell et al., 2012), which thus could be linked in some respect to the global

impacts of the A.D. 1257 ultraplinian Samalas eruption (Lavigne et al., 2013).

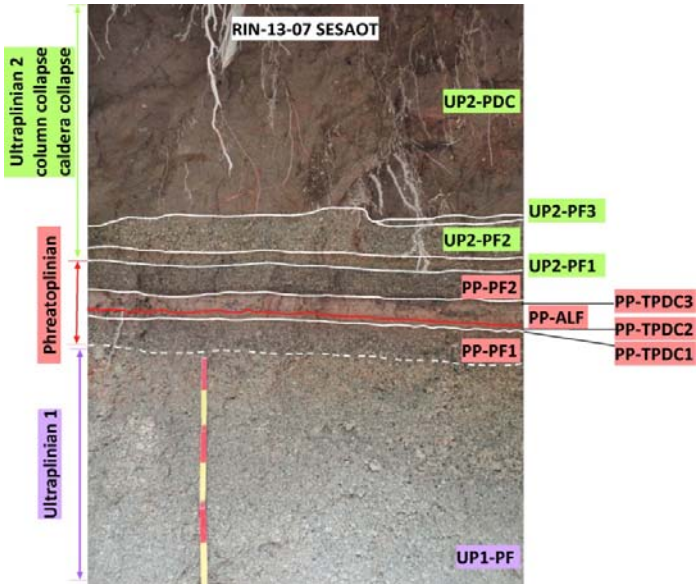

Fig. 14. Representative stratigraphy of AD 1257 Samalas eruption (RIN-1307, Sesaot, 22 km from source). See Fig. 16 for legend (Vidal et al., 2013; in prep.).

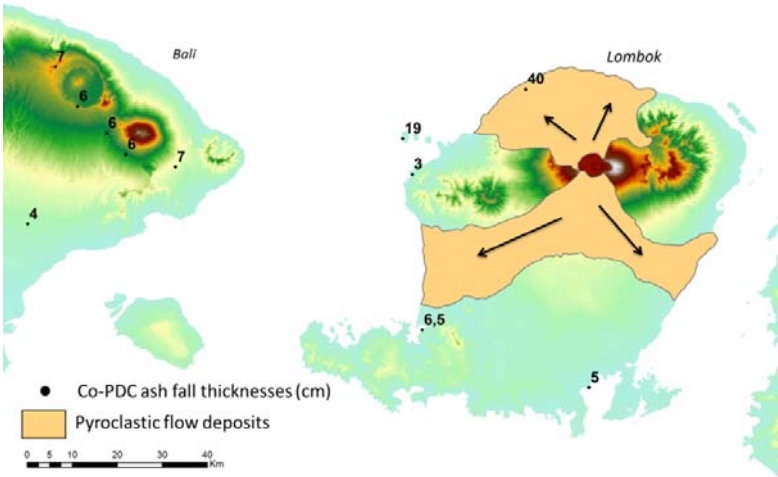

Fig. 15. Map of PDC emplaced on land during the AD 1257 eruption with thickness (cm) of associated co-PDC ash fall unit (Vidal et al., 2013; in prep.).

Preliminary analysis of medieval chronicles written by monks in France and Britain documents the occurrence of initial winter warming in the winter of 1258 just following the eruption, a phenomenon expected by climate models, that was followed by extensive wet and cold climatic conditions in 1259 (Delisle et al., 1877; Luard, 1872-1873), Giles (1854) which may have impacted crops and contributed to the onset and magnitude of famines at that times. The occurrence of these difficult climatic conditions, unexplained by rational thought at the time, might have contributed to the rise of the Flagellants (The Columbia Encyclopedia, 2013). This religious mouvement developed in the 13th and 14th century in medieval Europe as a group of practitioners who strongly advocated public self-flagellation and self-mortification as a form of fervent piety necessary to avoid acts of Godly punishement in the form of natural calamities, as a response to perpetual human sins. This mouvement manifested itself as oubreaks of popular passion, the first incident having occurred in AD 1259 in Perugia (Italy) the year after severe crop damage and famine occurred throughout Europe, and thus in AD 1258. The mouvement peaked during the period of the Black Death aroung the major epidemic of plague in Europe around 1347.

The AD 1257 caldera eruption of Samalas thus produced two sustained ultraplinian injections that released large amounts of fine ash, halogen and sulphur gases in the stratosphere. This eruption is thus similar in magnitude, intensity and style as the famous eruption of Tambora volcano on nearby Sumbawa island, whose paroxysmal phase occurred on 15 April AD 1815 with a magnitude of 7 (**Table 2**). However Samalas' sulfate spike recorded in ice cores and modelled SO_2 stratospheric loading much greater than that of Tambora (eg. Gao et al., 2008; Sigl et al., 2014). The AD 1257 eruption's sulfur loading might even have contributed to the onset of a trend of global cooling linked to a series of large medieval eruptions that occurred in a short time span and that culminated in the Little Ice Age (Miller et al., 2012). At the local and regional scales, the socio-economic and environmental consequences of this cataclysmic event must have been dramatic. Significant parts of Lombok, Bali, and the western part of Sumbawa were likely left sterile and uninhabitable for generations. This finding might provide insights as to the reasons why the Javanese King Kertanegara, who invaded Bali in A.D. 1284, did not encounter any resistance by local population (Lavigne et al., 2013). Analysis of the Babad Lombok also suggests the existence of the ancient capital of the Kingdom of Lombok, Pamatan, which was destroyed by the eruption and whose remains might lie several meters buried by the pumice fallout and pyroclastic flow deposits of the AD 1257 eruption. The potential discovery by future archaeological surveys of this Indonesian “Pompei” would constitute a regional and world heritage contribution of major cultural and historical importance.

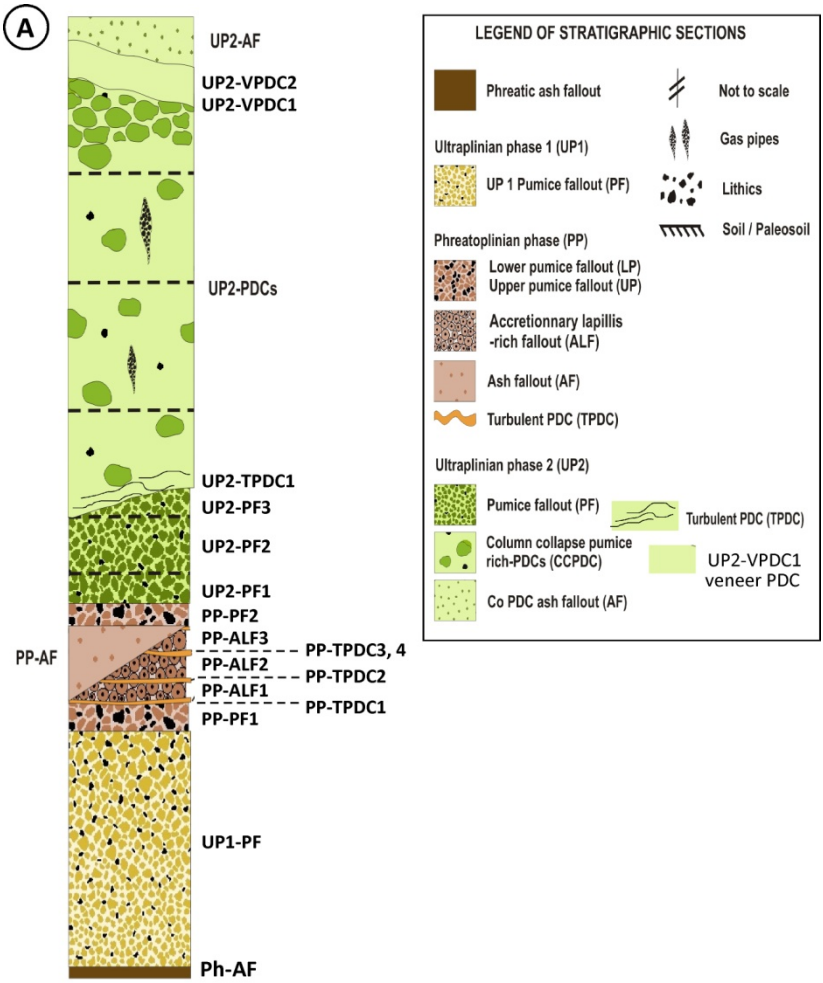

Fig. 16. Synthetic stratigraphy of the AD 1257 Ultraplinian Samalas eruption ((Vidal et al., 2013; in prep.)

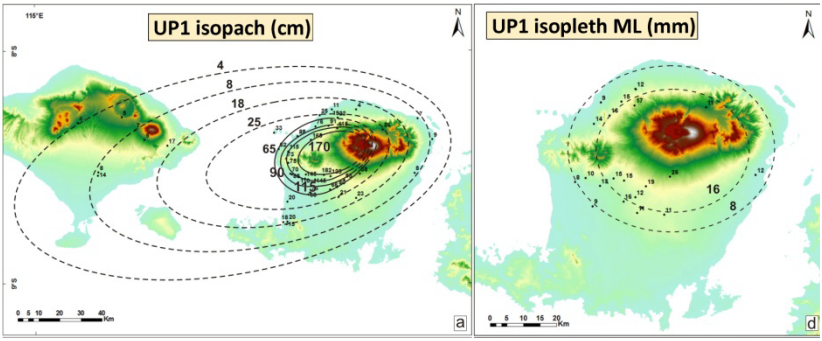

Fig. 17A. Distribution of first ultraplinian fallout unit, AD 1257 Samalas eruption (Vidal et al., 2013; in prep.).

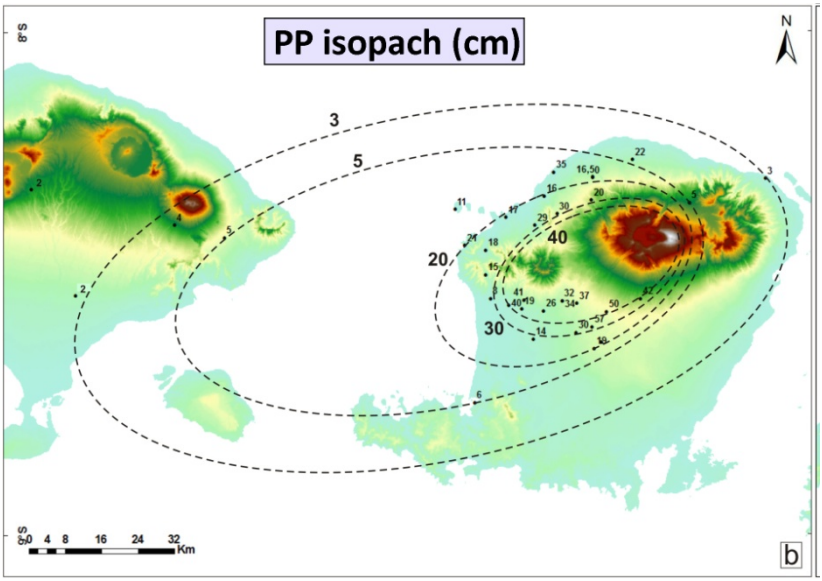

Fig. 17B. Distribution of phreatoplinian fallout unit, AD 1257 Samalas eruption (Vidal et al., 2013; in prep.).

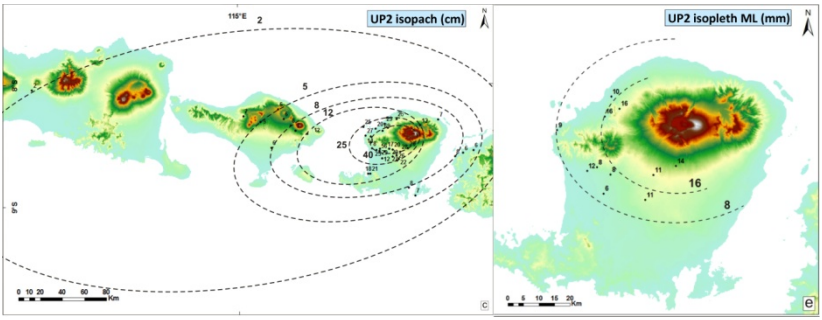

Fig. 17C. Distribution of second ultraplinian fallout unit, AD 1257 Samalas eruption (Vidal et al., 2013; in prep.).

Table 2. Characteristics of the largest well-documented volcanic eruptions (VEI > 5) during the Holocene (Taken from Lavigne et al., 2013).

Volcano	Country	Deposit name	Bulk deposit volume (km^3)	DRE volume (km^3)	Adjusted mass (kg)	Mass eruption rate (kg/s)	Maximum magnitude*	Intensity†	Age	Source
Kurile Lake	Kamchatka, Russia	KO	170	80	1.92×10^{14}		7.3		6460–6414 cal B.C.	(1)
Santorini	Greece	Minoan‡		60	1.48×10^{14}	2.50×10^{8}	7.2	11.4	1627–1600 cal B.C.	(2, 3)
Mazama (Crater Lake)	Oregon, United States	Lower pumice‡		52	1.28×10^{14}		7.1		5677 cal B.C.	(4, 5)
Samalas	**Indonesia**	**1257 A.D.‡ §**		>40	$\mathbf{9.90 \times 10^{13}}$¶	$\mathbf{1.10 \times 10^{9}}$	7.0	12.0	**Cal A.D. 1257**	**Present work**
Ilopango	El Salvador	Tierra Blanca Joven	84	39	8.15×10^{13}		6.9		Cal A.D. 536	(6. 7)
Tambora	Indonesia	A.D. 1815 ‡		>33	8.15×10^{13}	2.8×10^{8}	6.9	11.4	A.D. 1815	(8, 9)
Taupo	New Zealand	A.D. 180	105	35	8.00×10^{13}	1.10×10^{9}	6.9	12.0	A.D. 232 ± 5	(8, 10, 11)
Aniakchak	Alaska, United States	3430 B.P.		27	6.21×10^{13}		6.8		1645 B.C.	(12–14)
Changbaishan/ Baitoushan	China/North Korea	Millenium eruption	96	24.5	5.64×10^{13}		6.8		Cal A.D. 946	(15, 16)
Quilotoa	Ecuador	800 B.P.	21.3	18.7	4.22×10^{13}	2.00×10^{8}	6.6	11.3	Cal A.D. 1275	(17, 18)
Katmai - Novarupta	Alaska, United States	Valley of 10 000 Smokes	17	6.8	3.00×10^{13}	1.00×10^{8}	6.5	11.0	A.D.1912	(8, 19)
Krakatau	Indonesia	A.D. 1883	18–21	12.5	3.00×10^{13}	5.00×10^{7}	6.5	10.7	A.D. 1883	(8, 20)
Santa Maria	Guatemala	A.D. 1902	20.2	8.6	2.00×10^{13}	1.70×10^{8}	6.3	11.2	A.D. 1902	(8, 21)
Quizapu	Chile	A.D. 1932 plinian	9.5	4	9.72×10^{12}	1.50×10^{8}	6.0	11.2	A.D. 1932	(22)
Pinatubo	Philippines	A.D. 1991		5	1.10×10^{13}	4.00×10^{8}	6.0	11.6	A.D. 1991	(8)
Vesuvius	Italy	A.D. 79		3.25	6.00×10^{12}	1.50×10^{6}	5.8	11.2	A.D. 79	(8, 23)
Rungwe	Tanzania	Rungwe pumice	3.2–5.8	1.4	2.00×10^{12}	4.80×10^{6}	5.3	11.7	ca. 4000 B.P.	(24)
Huaynaputina	Peru	A.D. 1600 Stage I	7	2.6	1.30×10^{12}	2.40×10^{8}	5.1	1.4	A.D. 1600	(25)
Chichon	Mexico	Unit B 550 BP	2.8	1.1	1.05×10^{12}	1.00×10^{8}	5.0	11.0	Cal A.D. 1320–1433	(26)

*$M = \log_{10}$(erupted mass kg) − 7.
†$I = \log_{10}$(mass eruption rate kg/s) + 3.
‡Erupted mass is taken assuming an average of 2,470 kg·m^3 for the dense-rock equivalent (DRE) density like for Samalas and Tambora.
§Minimum magnitude as uncertainty on distal to very distal ash bulk volume is significant.
¶Minimum value, that of the calculated missing caldera.

1. Ponomareva VV, et al. (2004) The 7600 (14C) year BP Kurile Lake caldera-forming eruption, Kamchatka, Russia: Stratigraphy and field relationships. *J Volcanol Geotherm Res* 136(3-4): 199–222.
2. Sigurdsson H, et al. (2006) Marine investigations of Greece's Santorini volcanic field. *Eos* 87(34):337–348.
3. Friedrich WL, et al. (2006) Santorini eruption radiocarbon dated to 1627–1600 B.C. *Science* 312(5773):548.
4. Bacon CR (1983) Eruptive history of Mount Mazama and Crater Lake caldera, Cascade Range, USA. *J Volcanol Geotherm Res* 18(1-4):57–118.
5. Zdanowicz CM, et al. (1999) Mount Mazama eruption: Calendrical age verified and atmospheric impact assessed. *Geology* 27(7):621–624.
6. Dull R, et al. (2010) Did the TBJ Ilopango eruption cause the AD 536 event? American Geophysical Union, Fall Meeting 2010, December 13–17, 2010, San Francisco.
7. Brown RJ, Vallance JW, Houghton BF, Hernandez W (2013) The AD 536 Phreatoplinian eruption of Volcán Ilopango, El Salvador: physical character of ash-rich pyroclastic-density-current deposits and coeval ash aggregates. IAVCEI 2013 Scientific Assembly, July 20–24, Kagoshima, Japan; poster, 3W-3G-P2.
8. Pyle DM (2000) Sizes of volcanic eruptions. *Encyclopedia of Volcanoes*, eds Sigurdsson H, Houghton B, Rymer H, Stix J, McNutt S (Academic, San Diego), pp 263–269.
9. Self S, Gertisser R, Thordarson T, Rampino MR, Wolff JA (2004) Magma volume, volatile emissions, and stratospheric aerosols from the 1815 eruption of Tambora. *Geophys Res Lett* 31: L20608.
10. Wilson CJN, Walker GPL (1985) The Taupo eruption, New Zealand I. General aspects. *Philos Trans R Soc Lond A* 314(1529):199–228.
11. Hogg A, Lowe DJ, Palmer J, Boswijk G, Bronk Ramsey C (2012) Revised calendar date for the Taupo eruption derived by 14C wiggle-matching using a New Zealand kauri 14C calibration data set. *Holocene* 22(4):439–449.
12. Larsen JF (2006) Rhyodacite magma storage conditions prior to the 3430 yBP caldera-forming eruption of Aniakchak volcano, Alaska. *Contrib Mineral Petrol* 152(4):523–540.
13. Begét J, Mason O, Anderson P (1992) Age, extent and climatic significance of the c. 3400 BP Aniakchak Tephra, Western Alaska, USA. *Holocene* 2(1):51–56.
14. Pearce NJG, Westgate JA, Preece SJ, Eastwood WJ, Perkins WT (2004) Identification of Aniakchak (Alaska) tephra in Greenland ice core challenges the 1645 BC date for Minoan eruption of Santorini. *Geochem Geophys Geosyst* 5 (3):Q03005.
15. Horn S, Schmincke HU (2000) Volatile emission during the eruption of Baitoushan volcano (China/North Korea) ca. 969 AD. *Bull Volcanol* 61(8):537–555.
16. Xu J, et al. (2013) Climatic impact of the Millennium eruption of Changbaishan volcano in China: New insights from high-precision radiocarbon wiggle match dating. *Geophys Res Lett* 40(1):54–59.
17. Mothes PA, Hall ML (2008) The plinian fallout associated with Quilotoa's 800 yr BP eruption, Ecuadorian Andes. *J Volcanol Geotherm Res* 176(1):56–69.

Part 2: Description of stops visited during the excursion

Authors :

Jean-Christophe Komorowski [1], Céline Vidal [1], Nicole Métrich [1], Franck Lavigne [2], M. Nugraha Kartadinata [3], Indyo Pratomo [4], Oktory Prambada [3]

1) Institut de Physique du Globe de Paris – CNRS UMR7154, Université Sorbonne Paris-Cité, France
2) Université Paris 1 Panthéon-Sorbonne, Département de Géographie, and Laboratoire de Géographie Physique, CNRS 8591, France
3) Center for Volcanology and Geological Hazards Management (CVGHM), Geological Agency, Bandung, Indonesia
4) Geological Museum, Geological Agency, Bandung, Indonesia

The excursion will last from the evening of 14 September (Day 1) till the morning of 19 September (Day 6) as we will leave from Yogyakarta take the plane together and end the excursion on the evening of 18 September with a fairwell diner. Participants can leave on the morning of 19 September. We will thus spend 4 full days in the field including the hiking and overnight camping on the northern caldera rim.

The following Part II of this guidebook describes the outcrops that we will see in the field from Day 2 through Day 5 (**Fig. 18**). During Day 2 we will visit stops S-1 through S-5 and perhaps time permitting S-6. On Day 3 we will visit stops S-7 through S-10 and then drive to our overnight hotel stop at Senaru (601 m). On Day 4 we will hike a strenuous but very well marked trail to the camp site at 2641 m of elevation (net elevation gain of 2000 m and a walking distance of about 10.5 km one way) for an average time of 7-8 hours including lunch stops and brief resting stops. There are several resting stops with shelters named POS1 (915 m), POS EXTRA (1165), POS2 (1500 m), POS3 (2000 m), and the camp site (Plawangan / Senaru crater rim) on the north rim (2641 m) which is

at tha start of the trail going down the N rim of the caldera to the lake shore (2000 m). GIVEN TIME CONSTRAINTS WE WILL NOT GO DOWN TO THE LAKE SHORE INSIDE THE CALDERA. On Day 4 we will make only one official stop (S-11) going up above POS3. We can make additional stops around the camping area as we wish. On Day 5 we will wake up early and start our descend making 2 stops S-12, and S-13 going down to Senaru for the return distance of 10.5 km. It is best to do most stops going down and thus climb "straight" without losing time for additional geology stops to try to get a sunset view at the caldera rim and allow time for variable climbing times.

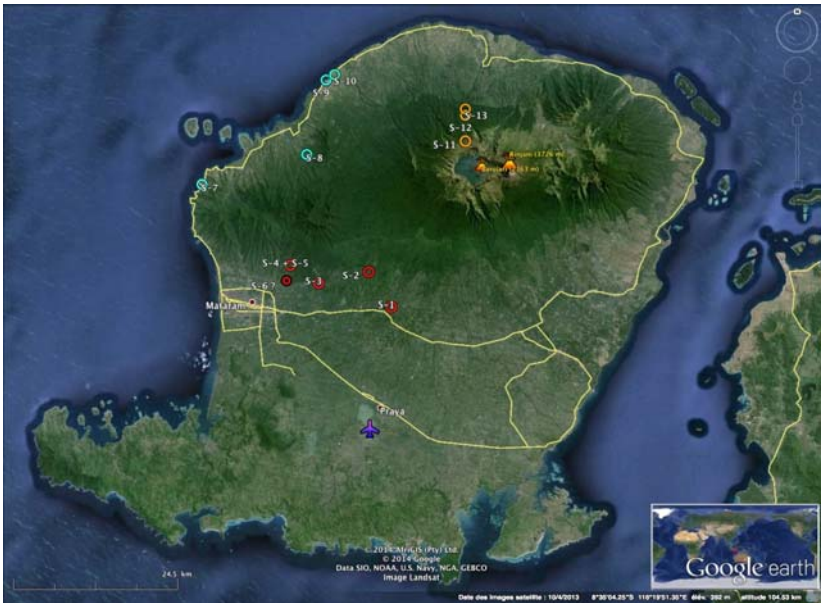

Fig. 18. Map of Lombok island with stops (S-1 to S-13) to be visited during the Rinjani COV8 excursion; Day 2 (red), Day 3 (blue), Days 4-5 (orange). Base map Google Earth.

Day 2

During Day 2 we will see and discuss the entire stratigraphy of the AD1257 Samalas ultraplinian eruption that is exposed in several outstanding outcrops to the southwest of the Segara Anak caldera of

the Rinjani volcanic complex at distances from about 22 to 33 km. Distances of outcrops to source are measured from the top of the active resurgent Barujari volcano inside the caldera. For information, the hotel where we will stay during the excursion in Senggigi is located 42 km west from Barujari crater.

From the hotel in Senggigi we will drive about 29 km east to the vicinity of the village of Pancardao, where we will start our way back west visiting 4 distinct areas (**Fig. 19).**

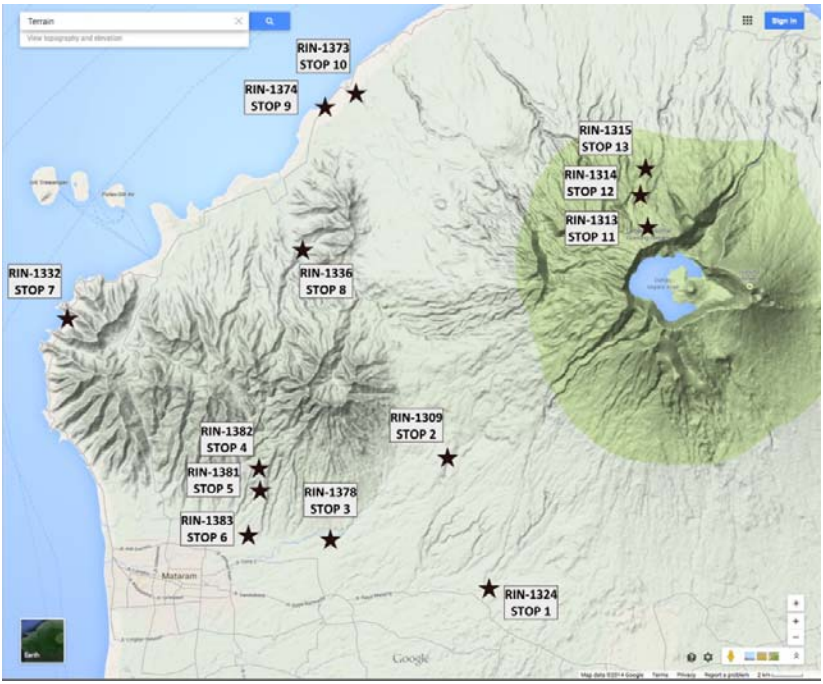

Fig. 19. Detail of shaded relief map of Lombok with stops (S-1 to S-13) to be visited during the Rinjani COV8, in darker green the Rinjani Regional Park area. North is up. Scale is in lower right corner of map. Base map from Google Maps.

Leave Senggigi at 8:30

STOP 1: RIN-1324 (Tanahembang)

Elevation: 331 m Distance to source: 24 km

Lat : S8°35‘18.2’’ Long : E116°18’12.2’’

Drive from Senggigi to Pancardao (29 km) on the road towards Masbagik and Selong. After reaching the town of Pancardao take a small road to the NE to an active quarry near Tanahembang in the valley.

In this active quarry, almost all stratigraphic units of the AD1257 eruption can be observed in detail and are very well exposed. In this oucrop we see about 13 to 25 m of AD1257 eruptive products resting on pre-eruption stratified fluviatile conglomerates and breccias of the Mataram paleobassin that reach several meters in thickness (**Fig. 22).** Here a thick sequence of AD1257 pumice-rich non-welded pyrolastic flows have mostly eroded the AD1257 pumice fallout units and filled the palleo-valley reaching a thickness of 12 to 20 m (**Figs. 20; 21).** They form a typical valley-filling flat topography where they have not been extracted for construction material. The area has been intensely cultivated and covered by rice fields.
From base to top we can see:

- A thick (≥ 1 m) paleaosoil horizon contains abundant organic material, burnt paleowood, and numerous archaeologic ceramic sherds from pre-AD1257 human occupation. The top of this unit is formed by a 2-3 mm iron.-rich oxydized reddish laminated unit very rich in non-burnt imprints of leafs and wood twigs.

- phase UP1, white pumice fall UP1-PF unit, 75-80 cm thick, reversely graded, poorly-sorted, rich in accidental clasts. The unit is very loose, massive but shows faint stratification due to sub-parallel alignment of dark particles (accidental clasts) and mafic crystals. Dark particles are more abundant towards the base. Contains pre-AD 1257 archaeologic ceramic.

- Phreatoplinian phase PP, gray pumice fall unit PP-PF1, 9 cm, normally graded, poorly sorted, very rich in dark juvenile and accidental clasts, better stratified. The layer is capped by a laminated, brownish 3 mm-thick, fine ash layer that is indurated due to iron oxidation.

- Phreatoplinian phase PP, unit PP-ALF, 14-38 cm thick, massive compact, blue-gray (hydrothermally altered material, reduced iron

sulfides e.g. pyrite ?), clay-rich, very fine ashfall unit, with very abundant, large, accretionary lapilli (up to 1.5 cm in diameter). This unit is not laterally continuous and is partly truncated by a basal and upper wavy-laminated fine sand-rich, moderately sorted, layers with ocre-orange oxidation coatings that show variable erosion into the lapilli ashfall layer. We interpret these wavy layers as distal dilute pyroclastic density current (surges) deposits (PP-TPDC-1 & 2) associated with the phreatoplinian phase. This PP unit contains abundant solidified casts of wood fragments as well as abundant burnt dark wood fragments.

- Phreatoplinian phase PP, gray pumice fall unit PP-PF2, 5-10 cm thick, moderately sorted, composed of a mixture of whitish pumice and darker juvenile clasts. The unit is weakly stratified given that it was emplaced on a slope. It also shows some pinching and swelling perhaps as a result of post-emplacement loading by the thick overlying pyroclastic density current pumice flow deposits (PDCs).

- Ultraplinian phase UP2, white pumice fall unit UP2-PF1, 9-27 cm thick, reversely graded, poorly-sorted but better sorted than unit UP1-FP, poor in accidental clasts . This unit is rich in charcoal fragments. It was strongly eroded by overlying PDCs as evidenced by injection of the basal part of the PDC (UP2-TPDC1) into the top of unit D.
  Ultraplinian phase UP2, sequence of several flow units of valley-ponding pumice-rich non-welded pyroclastic density current deposits (UP2-PDCs). The base of the lowermost PDC flow unit is an indurated, wavy stratified, 10-13 cm thick unit (unit UP2-TPDC1) that contains locally some rounded pumice clasts. This unit has eroded into the underlying pumice fallout unit UP2-PF1. The contact between the basal part of the PDC and the fallout is a laminated 1-3 mm thick black carbon-rich undulating indurated tar layer that we interpret as evidence for the massive burning of paleo-forest by PDCs as has been documented elsewhere (e.g. Scott et al., 2008; Bull et al., 2008; Sparks et al., 2002; Voight et al., 2002). This basal unit UP2-TPDC1 is interpreted as having been deposited from a more dilute stratified high-energy current (ground layer). Several of the PDC units show large (>20 cm) floated pumice at the unit top or forming pumice lenses within the unit. The presence of u-shaped channels in the PDC units with different orientations suggests that

PDCs interacted with pre-eruption topography and the early flows followed several pre-eruption river channels with different orientations.

Fig. 20. Stop 1: full stratigraphy of the AD1257 ultraplinian eruption. Notice blue-gray PP unit full of accretionary lapilli above the UP1 whitish puice fallout unit overlying the brown organic-rich paleosoil horizon at the base. Notice the thick sequence of pumice-rich non-welded pyroclastic density current flow deposits.

Fig. 21.. Stop 1: Overview of the cummulative thickness (12-20 m) of the UP2 phase pumice-rich non-welded pyroclastic density current flow deposits.

STOP 2: RIN-1309 (Labahsempaga)

Elevation: 327 m	Distance to source: 22 km
Lat : S8°32‘31.5’’	Long : E116°16’23.9’’

Drive back from Stop 1 to the main road to Pancardao and follow it in direction of Narmada and Mataram for 5 km towards the west. At the entrance of Sedau, take a road going north towards Sesaot and drive 6 km until reaching Labahsempaga. Stop 2 is at the bottom of Kokok Kumbi river valley accessible from the quarry at the top where an aqueduct was built in the upper part of the overhanging cliff.

This is one of the most impressive sites where the full AD1257 stratigraphy can be seen at Stop 1. The sequence of pumice-rich pyroclastic flows from the UP2 ultraplinian and caldera collapse phase are beautifully exposed along a very recent and fresh vertical cliff and reach at least 47 m, one of the greatest thicknesses of the entire area (**Fig. 22**). They form a perfect typical valley-filling flat-topped topography. This sequence rests on earlier eruptive units of the PP and UP1 phases as described in Stop 1. Stop 2 shows one of

the most impressive set of depositional lithofacies of the phreatoplinian phase PP of the AD1257 eruption.

Compared to Stop 1, the greatest differences in the stratigraphy concern the PP phreatoplinian phase. Here the PP phase lacks its pumice fallout units PP-PF1 and PP-PF2 but is characterized by a significant developpment of the accretionary lapilli-bearing blue-gray clay-rich (hydrothermally altered material, reduced iron sulfides e.g. pyrite ?) fine ash-layers that are intercalated with several thin distal dilute turbulent PDC deposits (**Fig. 22).** Overall the other units that are present in both Stop 1 and 2 show similar sedimentological characteristics. From base to top we observe:

- Thick sequence (5-15 m) of older pre-AD1257 volcaniclastic deposits with rounded lava boulders (e.g. colluvium, redish clay-rich debris flow deposits) and possible pyroclastic flow deposits.

- Ultraplinian phase UP1, very vesicular white pumice fall unit UP1-PF, 125 cm thick, rich in accidental clasts, deposited on gentle slope.

- Phreatoplinian phase PP, unit PP-ALF, 50 cm thick, massive compact, blue-gray clay-rich, very fine ash fall unit with very abundant accretionary lapilli (up to 0.5-1 cm in diameter). This unit consists of several layers PP-ALF1 (4 cm), PP-ALF2 (17 cm), PP-ALF3 (16 cm) that are intercalated and partly truncated by several wavy-laminated fine sand-rich, moderately-sorted, layers of variable thickness with ocre-orange oxidation coatings that show variable erosion into the accretionary lapilli ashfall layers. The wavy layers are richer in accidental clasts but contain scattered 1-4 cm sized armored pumice clasts (ie. pumice core coated with concentric laminae of blue-gray fine ash). We interpret these wavy layers as erosive distal dilute pyroclastic density current (surges) deposits (PP-TPDCs) associated with the phreatoplinian phase.

- Ultraplinian phase UP2, white less vesicular pumice fall unit UP2-PF1, 20 cm thick, poor in accidental clasts, weakly stratified.
  Ultraplinian phase UP2, sequence of several units (UP2-PDCs) of valley-ponding non-welded pyroclastic density current deposits (PDCs) reaching a cumulative thickness of 47 m. The basal contact of the PDC sequence is formed by a conspicuous 0.5-1 cm thick, finely laminated fine sand to ash-rich indurated layer (UP2-TPDC1),

that is very rich in organic dark material with wavy bedding. This basal unit is interpreted as having been deposited from a more dilute stratified high-energy current (ground layer) that caused very rapid wholesale combustion of the pre-eruption vegetation and formation of a carbon-rich aerosol that settled to form this tar layer (e.g. Scott et al., 2008; Bull et al., 2008; Sparks et al., 2002; Voight et al., 2002). The lowermost PDC unit is very rich in white pumice and contains abundant black unaltered obsidian clasts. The overlying remaining series of valley-ponding indurated but non-welded PDCs units are relatively poor in pumice clasts at this location. Perched paleo-thalweg channels formed after the eruption by the renewal of fluviatile incision of the PDCs can be seen in the upper part of the sequence.

Next page:

***Fig.** 22. Stop 2: Full stratigraphy of the AD1257 Samalas eruption in Kokok Kumbi river valley near Lebahsempaga. A-B: General view of the valley from top and from bottom. C-D: Detail of the phreatoplinian blue-gray ashfall unit with large accretionary lapilli with intercalated ocre-colored thin dilute pyroclastic density current deposits; E: Black organic tar layer from massive combustion of the pre-eruption forest on top of the ultraplinian phase UP2 pumice fallout unit UP2-PF1.*


A
B
C
D
E

STOP 3: RIN-1378 (Punikan)

Elevation: 142 m Distance to source: 29 km
Lat : S8°33‘25.3’’ Long : E116°12’22.6’’

Drive back from Stop 2 to Sedau for 6 km to the main Narmada-Matarama road. Turn west towards Mataram and drive until Narmada. Turn North at Narmada towards the mountains for 3-4 km on a small road until you reach Punikan. Stop 3 is an active quarry and clay brick factory just above the valley of the meanders of the Kokok Jankok River flowing from east to west.

This is a very nice active quarry that exposes at least ≥ 13 m of the main stratigraphic units of the AD1257 eruption. At this location the ultraplinian pumice fallout units UP1 and UP2 and the pumice fallout units of the phreatoplinian phase PP are more complete and well preserved despite the presence of thick overlying valley-ponding flat-topped pumice pyroclastic flow deposits of the UP2 ultraplinian caldera-collapse phase. This is thus an interesting location showing that the erosive effects of the pyroclastic flows from the UP2 column collapse phase were less pronounced than at other locations. The succession of several pumice fallout layers within the UP2 ultraplinian phase with varying sedimentologic characteristics and limited thickness strongly suggests that the eruptive column had become unstable and mass flux was fluctuating, heralding the wholesale column collapse phase and caldera formation with emplacement of widespread thick non-welded pyroclastic flows. This location allows us to observe the eruptive dynamics just prior caldera formation. Overall, the other units that are present in Stop 3 show similar sedimentological characteristics as in Stop 1 and 2. From base to top we observe:

- Thick sequence (? m) of older pre-AD1257 silt and clay-rich paleosoil horizon used for the brick factory.

- Ultraplinian phase UP1: very vesicular white pumice fall unit UP1-PF, 145 cm thick, reversely graded, rich in accidental clasts, faintly stratified.

- Phreatoplinian phase PP, gray pumice fall unit PP-PF1, 12 cm, poorly sorted, very rich in dark clasts.
- Phreatoplinian phase PP, unit PP-ALF is 8.5 cm thick and consists of three layers: a 4.5 cm thick, compact, brownish, fine ashfall layer (PP-ALF1) rich in accretionary lapilli, as well as rounded pumice clasts overlain by a 0.8 cm thick layer (PP-TPDC) that shows variable thickness and thickens in hollows and consists of lenses of fine pinkish ash thinly laminated. We interpret PP-TPDC as having been emplaced by distal dilute pyroclastic density currents (surges) associated with the phreatoplinian phase). PP-TPDC is capped by a 3.2 cm thick layer of extremely well-sorted fine to coarse sand, clast-supported fallout consisting of abundant dark juvenile clasts.

- Phreatoplinian phase PP, gray pumice fall unit PP-PF2, 7 cm thick, normally graded, better sorted than PP-PF1, composed of a mixture of whitish pumice and darker juvenile and accidental clasts. This unit is capped by a dark, oxidized and thinly laminated, indurated layer.

- Ultraplinian phase UP2, white to pinkish pumice fall unit UP2-PF1, 3 cm thick, reversely graded, less accidental rich than B2.

- Ultraplinian phase UP2, white pumice fall unit UP2-PF2, 8.5-9.5 cm thick, normally graded, ends with pinkish oxidation stains.

- Ultraplinian phase UP2, white to pinkish pumice fall unit UP2-PF3, 13.5 cm thick, non- to reversely graded, poor in accidental clasts, poorly sorted.

- Ultraplinian phase UP2, lenticular 4-12 cm thick unit (UP2-TPDC) that is compact, very poorly sorted and contains abundant rounded pumice. This unit has eroded into the underlying pumice fallout unit UP2-PF3. This unit is capped by a wavy-bedded, finely laminated, fine ash rusty-colored layer (0.5-0.8 cm) with rounded pumice clasts. We interpret this 2-layer unit as having been deposited from a more dilute stratified high-energy current perhaps associated with the overspill lobe of a pumice-rich pyroclastic flow.

- Ultraplinian phase UP2, sequence of several flow units of valley-ponding pumice-rich and ash-rich pinkish non-welded pyroclastic density current deposits (UP2-PDCs) reaching ≥ 13 m in thickness.

The uppermost units are less rich in pumice and have a darker colored matrix.

STOP 4: RIN-1382 (Leong)

Elevation: 264 m	Distance to source: 31 km
Lat : S8°31‘59.5’’	Long : E116°10’06.0’’

Drive back from Stop 3 to the town of Pemangkalan, then drive N-NW to cross the Kokok Jangkok river and drive west on the road through Longseran Timur for about 5 km until you reach the village of Langko. Take a road going uphill N to Leong. Drive for about 3.5 km past Leong to the next village, that is perched above the valley where the Kokok Bukit river splits in two smaller valleys uphill. Stop 4 is a viewpoint where we can see some interesting interaction of the PDCs with the topography.

The N-S valley of the Kokok Bukit river runs perpendicular to the general direction taken by the main column collapse PDCs of the UP2 ultraplinian phase that radiated from the Samalas caldera and thus were traveling here from East to West. Here we notice in the fields all around an upper pinkish brown colored fines-rich ca. 150 cm thick deposit that has a variable thickness, is thicker in hollows and contains rounded white pumice. This deposit forms a veneer on the topography of ridges and the slopping flanks of the older caldera complex of Gunung Meninting (1418 m). It rests above the UP2-PF1 unit pumice fallout unit described at stop 5.

We interpret this deposit to have formed as a result of the “secondary” sedimentation of large radiating ashclouds that were associated with emplacement of widespread caldera-collapse pumiceous non-welded pyroclastic density currents that we have seen at stops 1, 2, and 3. These PDCs were radiating from the caldera until they interacted with major topography formed by Gunung Meninting that rises nearly 1000 m above the lower western flanks of Rinjani. The secondary PDCs took different directions. This process would be analogous, albeit on a much larger scale, to the secondary PDCs described by Druitt et al. (2002) in Dry Ghaut for

the Boxing Day 26 December 1997 eruption of Soufrière Hills (Montserrat).

STOP 5: RIN-1381 (Leong)

Elevation: 241 m Distance to source: 31 km
Lat : S8°32‘07.6’’ Long : E116°10’02.1’’
Drive back south from Stop 4 for about 1 km or less along the ridge. Stop 5 is an active quarry/construction site on the West side of the road.

This is an impressive outcrop of the pumice fallout units from the two ultraplinian phases UP1 and UP2 separated by the phreatoplinian PP phase. This outcrop is located down axis and at medial distances on land from the source and showing some of the greatest thicknesses. The units were emplaced on a low sloping hill much higher than the valley bottom where the thickest column collapse and caldera collapse PDCs where emplaced. From base to top we observe:

- Pre-AD1257 paleosoil horizon.
- Ultraplinian phase UP1: very vesicular white pumice fall unit UP1-PF, 172 cm thick (one of the largest thicknesses of our current study), reversely graded, moderately sorted with some large scattered pumice clasts, rich in accidental clast which show an upward enrichment, salt & pepper appearance, grading into unit PP-PF1.
- Phreatoplinian phase PP, gray pumice fall unit PP-PF1, 7-8 cm, non graded, very poorly sorted, very rich in accidental dark clasts, finer grained than unit UP1-PF.
- Phreatoplinian phase PP, unit PP-TPDC is 6-22 cm thick with a characteristic variable and undulating thickness, brownish fine sand, contains accidental and sub-rounded pumice clasts towards the base and an erosion lowermost contact with the underlying B2 fallout unit. We interpret this unit as having been emplaced by distal dilute pyroclastic density currents (surges) associated with the phreatoplinian phase PP.

- Phreatoplinian phase PP, gray pumice fall unit PP-PF2, 11 cm thick, normally sorted, less coarse than PP-PF1, contains accidental dark clasts.

- Ultraplinian phase UP2, yellowish pumice fall unit UP2-PF3, 28-29 cm thick, normally graded, poorly sorted, poor in accidental clasts, some dark clasts but less of a salt & pepper appearance than unit UP1-PF.

STOP 6: RIN-1383 (Leong)

Elevation: 129 m Distance to source: 33 km
Lat : S8°33‘08.4’’ Long : E116°09’49.8’’

Drive back south from Stop 5 for about 2 km or less along the ridge. Stop 6 is in the construction site of a new blue Mosk on the East side of the road. This is an impressive outcrop showing about 35 m of exposure oriented East-West sub-parallel to the main tephra dispersal axis and 33 km down wind from the source. The outcrop is on the same interfluve gently sloping from the summit of the of the Gunung Meninting (1418 m) volcanic complex.

A series of at least three U-shaped channels that eroded into UP1 and upper PP units are beautifully exposed. The axes of the channels are oriented nearly N-S with N5°W-N6°E and N2°W-N6°E (declination set 13°W). This orientation is perpendicular to the East-West direction of the main caldera-collapse PDCs that radiated west from the caldera and that we have seen at STOP 3 and that have left at STOP 4 a pinkish veneer PDC deposit. The channel was eroded into the PP-PF1 pumice fall unit and was filled with fine ash unit with irregular thickness that we interpret as unit PP-TPDC. The channel is then filled by the remainder of the pumice fallout units of the PP and the UP2 phases that we have described before. The channel occurred during the phreatoplinian PP phase. From base to top we observe:

- Ultraplinian phase UP1: very vesicular white pumice fall unit UP1-PF, ≥ 145 cm thick, reversely graded, moderately sorted with some large scattered pumice clasts, rich in accidental clasts, faintly stratified and locally eroded by unit PP-TPDC.

- Phreatoplinian phase PP, gray pumice fall unit PP-PF1, 5 cm, was almost entirely eroded by unit C and is only present in the areas outside of the channel.

- Phreatoplinian phase PP, unit PP-TPDC is 8-16 cm thick with a characteristic variable and undulating thickness, brownish fine ash to sand, contains accidental and sub-rounded pumice clasts towards the base, shows a strongly erosive lowermost contact with the underlying PP-PF2 and UP1-PF fallout units. We interpret these U-shape channels to be erosional furrows caused by the emplacement of dilute pyroclastic density currents of the PP phreatoplinian phase that were deflected upon their interaction with the Gunung Meninting steep and high topography that might have provided additional potential energy for the dilute PDCs that were capable overpassing it. The PDCs were able to re-condense and likely experienced a second collapse from the liftoff cloud that formed above the high topography (Druitt et al., 2002). The collapsing PDCs then flowed partly confined by the deep valleys on the flanks of the Gunung Meninting volcanic complex. These dilute PDCs thus occurred before the caldera-collapse phase.

- Phreatoplinian phase PP, gray pumice fall unit PP-PF2, 13-14 cm thick, normally sorted, less coarse than PP-PF1. Unit was overthickened in the deepest part of the channel due to emplacement on steeper inner channel slope.

- Ultraplinian phase UP2, pinkish pumice fall unit UP2-PF1, 9 cm thick, reversely to non graded, poorly sorted, rich in accidental clasts. Although unit UP2-PF1at STOP 3 is not rich in accidental clasts, the stratigraphic position of this unit here at STOP 6 suggests that it is correlative with unit UP2-PF1 at STOP 3 and represents the first unit of the UP2 ultraplinian phase.

- Ultraplinian phase UP2, gray pumice fall unit UP2-PF2 12 cm thick, normally graded, less sorted than D, rich in accidental clasts. Ultraplinian phase UP2, pinkish pumice fall unit UP2-PF3 35 cm thick, reversely to non-graded, poorly sorted, rich in accidental clasts.

DAY 3

Leave Senggigi at 8:30

STOP 7: RIN-1332 (Nipah)

Elevation: 9 m	Distance to source: 41 km
Lat : S8°25‘34.8’’	Long : E116°02’58.6’’

From Senggigi we will drive along the coast of the Sea of Bali to the North for about 11 km in the direction of the village and Pemenang until we reach the second cove North of the Mt Agung viewpoint (Pemenang if the turn off for the village of Bangsal where the ferry for the Gili islands can be taken). STOP 7 is located on the north side of the Nipah cove (Teluk Nipah), about 300 m from the beach.
This is another interesting outcrop located roughly along the main tephra dispersal axis, 41 km from the source. This area is located West on the other side of the large Gunung Meninting (1418 m) volcanic complex. Here we can observe how dilute and more concentrated PDCs from the UP2 ultraplinian and caldera collapse phase UP2 interacted with topography and with the underlying ultraplinian UP1 and phreatoplinian PP phase fallout deposits. From base to top we see:

- Pre-AD1257 paleosoil horizon

- Ultraplinian phase UP1: very vesicular white pumice fall unit UP1-PF, 62 cm thick, reversely graded, poorly sorted, weakly stratified with pumice trains (sloping substratum), the base of the unit (first 17 cm) is very well sorted, finer grained and richer in dark accidental and juvenile fragments although unit A overall is less rich in large accidental clasts as observed elsewhere, grades into the overlying PP-PF1 unit.

- Phreatoplinian phase PP, gray pumice fall unit PP-PF1, 6 cm, better sorted and less stratified than unit UP1-PF, very rich in accidental clasts.

- Phreatoplinian phase PP, is 6.8-19 cm thick and composed of 5 layers: 1) layer PP-ALF1, is 1.5-2 cm thick and composed of compact brownish-beige colored fine ash (fallout), contains small pumice clasts and accretionary lapilli; 2) layer PP-TPDC1 is 0.8-2.5

cm thick, compact, dark grey, very well-sorted coarse ash, rich in dark accidental clasts, the layer is laterally continuous and has a very sharp lower contact with unit PP-TPDC1 but it show some thickening in hollows which suggest that it was emplaced from a dilute turbulent distal PDC; 3) layer PP-TPDC2 is 3-9 cm thick, less compact, poorly sorted, fines depleted, rich in accidental and pumice small lapilli, laterally less continuous than PP-TPDC1 showing pinch and swell lenticular bedding structures and erosive structures into underlying PP-TPDC1 layer, we interpret PP-TPDC2 as having been emplaced by distal yet more energetic dilute turbulent and erosive PDCs of the phreatoplinain PP phase; 4) layer PP-AF is 0.5 to 2.5 cm thick, compact, dark grey, very well-sorted coarse ash rich in dark accidental clasts that is coarser than PP-ALF1 (fallout); and 5) a pinkish fine ash compact PP-TPDC3 layer with small oxidized pumice clasts, 1 to 3 cm thick that is uneven in thickness and erosive into the underlying PP-ALF1 unit and that we thus interpret as having been emplaced by dilute turbulent and erosive PDCs of the phreatoplinain PP phase.

- Phreatoplinian phase PP, gray pumice fall unit PP-PF2, 6 cm thick, moderately reversely graded, poorly sorted, finely stratified rich in small size accidental clasts, laterally continuous.

- Ultraplinian phase UP2, pinkish pumice fall unit UP2-PF1, 24-27 cm thick, normally graded, poorly sorted, poor in accidental clasts, coarser than unit UP1-PF, upper contact is undulating due to erosion by overlying unit.

- Ultraplinian phase UP2, pinkish unit UP2-VPDC1, 12 cm thick, poorly sorted, fine ash with some pumice, variable thickness and laterally discontinuous, shows an undulating erosive contact into the lower unit UP2-PF1, interpreted as a distal veneer high energy dilute PDC that overpassed the topography of the old volcanic complex and recondensed as secondary PDCs that flowed along the slopes towards the sea.

- Ultraplinian phase UP2, light tan to whitish, very well sorted fine ash-rich unit UP2-AF, 11-27 cm thick, interpreted to be a co-PDC fine ash fallout unit, showing eroded contact with underlying unit UP2-VPDC1.

- Ultraplinian phase UP2, compact grayish brown, fine ash-rich UP2-VPDC2 unit, 11-27 cm thick, with rounded pumice, thickens in lows, showing erosive contact with underlying unit with some rip-up clasts of unit UP2-AF, reversely to non graded, poorly sorted, rich in accidental clasts, interpreted as a distal veneer secondary PDC (less dilute than unit UP2-VPDC1) that overpassed the topography of the old volcanic complex and recondensed to flow along the slopes towards the sea.

- Reworked wavy-bedded well-sorted sandy, cross-stratified gray fluviatile deposits, 5-10 cm thick

- Reworked pumice-rich debris flow

STOP 8: RIN-1336 (Dasanbanget)

Elevation: 51 m Distance to source: 26 km
Lat : S8°23‘11.2’’ Long : E116°11’24.7’

From STOP 7 continue to drive N-NE towards Pemenang (8 km) and Tanjung (9 km). In Tanjung turn right towards Lendangbila and drive 5 km South along the Kali Segara River on a small road to the villages of Gelumpang and Dasambaro. STOP 8 is in Dasanbangket, not far from the mosk in a new cut behind a house.

This stop shows much better the features we have discussed at STOP 6 and which we also discussed at STOP 7. Indeed here we observe how dilute and more concentrated PDCs from the UP2 ultraplinian and caldera collapse phase UP2 interacted with topography and with the underlying ultraplinian UP1 and phreatoplinian PP phase fallout deposits. The outcrop face is oriented roughly East-West and an angle to PDC flow direction. This location is located West of some important topographic ridges that stood in the way of PDCs from the eruption originating at the caldera and traveling West. From base to top we see:

- Pre-AD1257 paleosoil horizon.

- Phreatic phase Ph: very fine-grained gray ash unit Ph-AF (2-3 cm thick) rich in accidental clasts below a carbon-rich black laminae.

- Ultraplinian phase UP1: very vesicular white pumice fall unit UP1-PF, 168 cm thick, reversely graded, poorly sorted, weakly stratified with pumice trains (sloping substratum), the base of the unit (first 26 cm) is better sorted sorted, finer grained and richer in dark accidental and juvenile fragments, grades into the overlying PP-PF1 unit. This unit is locally eroded by U-shaped channels that were formed by distal dilute high-energy PDCs.

- Phreatoplinian phase PP, gray pumice fall unit PP-PF1, 7-8 cm, better sorted finer grained than unit UP1-PF, very rich in accidental clasts. This unit is locally eroded by U-shaped channels that were formed by distal dilute high-energy PDCs.

- Phreatoplinian phase PP, this unit is 6.8-19 cm thick and composed of 4 layers: 1) layer PP-TPDC1, is 2-3 cm thick and composed of compact brownish-beige colored fine ash that contains small pumice and accidental clasts and accretionary lapilli, locally thinly laminated, thicker in topographic lows and thinner on crests, strongly erosive into underlying units, characterized by a marked wavy bedding (**Fig. 23**) with wavelengths of 1.4 to 4 m, wave heights of 11 to 40 cm, and crest axes oriented N11°W, N15°W, N26°W, and N36°E (declination set 13°W); we interpret this unit as having been emplaced by distal yet energetic dilute turbulent and erosive PDCs of the phreatoplinian PP phase that were formed as a result of interaction of PDCs with the local topography that caused secondary sedimentation and refocusing of the PDCs; 2) layer PP-AF is 4-5 cm thick, massive, compact, brownish beige, rich in fine ash layer (fallout) that contains small pumice clasts, the base and top of this layer are formed by oxidized rust-colored hardened laminae; 3) layer PP-TPDC2 is 10-13 cm thick, loose, moderately sorted, fines depleted, rich in accidental and pumice small lapilli, showing some local stratification, thicker in topographic lows and thinner on crests; we interpret PP-TPDC2 as having been emplaced by distal dilute turbulent and erosive PDCs of the phreatoplinian PP phase; 4) layer PP-TPDC3 is 10-14 cm thick, normally graded, poorly sorted, massive, fines-poor, contains rounded pumices that are aligned along their platy axis, and shows planar to wavy stratification, the lower part is pinkish and was oxidized by the underlying unit ; we thus interpret as having been

emplaced by dilute turbulent and erosive PDCs of the phreatoplinain PP phase.

- Ultraplinian phase UP2, gray pumice fall unit UP2-PF1, 26-55 cm thick, normally graded, poorly sorted, loose, poor in accidental clasts compared to unit A, weakly stratified, contains charcoal wood casts and evidence of significant erosion by overlying unit.

- Ultraplinian phase UP2, pinkish brown compact unit UP2-VPDC2, 25 cm thick but variable, poorly sorted, rich in fine ash with rounded pumice that are aligned along their platy axis, variable thickness and laterally discontinuous, shows an undulating erosive contact into the lower unit UP2-PF1, interpreted as a distal veneer less turbulent and more concentrated PDC that overpassed the topography of the old volcanic complex and recondensed as secondary PDCs that flowed along the slopes of the ridges.
  Reworked thick (> 1 m) wavy-bedded, well-sorted sandy, cross-stratified gray fluviatile deposits as well as remobilized pumice fallout by surface runoff on steep slopes.

Fig. 23. Stop 8: Large-scale well-preserved wavy bedding (crests and throughs) formed by emplacement of secondary dilute turbulent PDCs that interacted with local topography during the phreatoplinian phase PP and that have eroded into UP1 and early PP pumice fall units. Wood measuring stick is 1.7 m.

STOP 9: RIN-1374 (Luk, Bali sea coast, Luk river)

Elevation: 0 m	Distance to source: 27 km
Lat : S8°17‘16.6’’	Long : E116°12’56.6’’

From STOP 8 drive back 5 km to the main road in Tanjung and turn right towards the East on the main road in the direction of Karanganyar, Kayangan, and Senaru further. Drive 13,2 km from

Tanjung until you reach the village on Montongpal, turn left at the second curve in the road (North) on a small dirt road and drive 300 m to the beach. Walk to the left to the beach and along the cliffs to STOP 9, south of the mouth of the Luk River.

BEWARE OF UNEXPECTED COLLAPSES OF LARGE VOLUMES (a few m^3) OF LOOSE MATERIAL FROM THE 35 M TALL CLIFF, DO NOT STAY LONG DIRECTLY BELOW THE CLIFFS. SCRAPE AND SAMPLE DEPOSITS CAREFULLY.

This is an outstanding beautifully exposed outcrop along the coastal sea cliffs where we can observe up to 35 m of pumice-rich non-welded PDC deposits. They were formed when pyroclastic flows of the ultraplinian UP2 column collapse and caldera formation phase entered the sea of Bali during the final phase of the AD1257 eruption. The PDCs traveled and completely filled the Luk River forming a pyroclastic delta at the coast. They created an inverse topography and the post-eruption Luk River has re-incised the pyroclastic PDC fan creating a new meandering channel offset from the pre-eruption thalweg. Upon entering the sea the PDC generated violent phreatomagmatic explosions that produced a series of numerous base surge turbulent density currents that jetted in a pulsating manner from the sea entry point carrying pumiceous and accidental pyroclastic material that accumulated to build a large pumice littoral cone (Furukawa et al., 2005; 2014; Lavigne et al., 2013).

The cliff face shows beautiful typical wavy bedding and cross-stratification with wavelengths of 1-2 m, as well as very well-developed planar bedding which gives the deposits a marked stratification (**Fig. 24**).

Fig. 24. Stop 9: Secondary phreatomagmatic dilute turbulent PDCs (surges) wavy bedded deposits in littoral pumice cone formed when collumn collapse pumiceous PDCs from the AD 1257 eruption of Samalas-Rinjani reached the northern coast of Lombok near the village of Luk.

The accidental clasts are diagnostically oxidized and form trains of clasts aligned in a sub-parallel manner. It is likely that following the deposition of the PDC, secondary explosions continued for a long time as the coastal wave action eroded the deposits exposing the hot PDC interior to the seawater. So far we have not found evidence nearby of a major tsunami linked to the entrance of these PDCs into the water following the AD1257 eruption. The entry of voluminous pumice flows into the sea produced extensive lasting and thick pumice rafts that must have covered a very wide area in the Sea of Bali and Java. We have seen evidence of pumice raft deposits on small islands just offshore from the northeast of Lombok (Gili Lawang, Gili Surat).

On the Eastern part of the cliff, towards the river, it is possible to observe a thick chaotic cobble-rich and tan-colored ash-rich deposits

with large pieces of coral that lies below a well-marked unit consisting of tan very fine and very well sorted ash that is the AD1815 Tambora caldera plinian eruption co-ignimbrite ashfall deposit (**Fig. 25**). This chaotic unit is interpreted (P. Wassmer, personnal communication, 2013) to represent the tsunami deposit on Lombok caused by the entry of pyroclastic flows from the 11 April AD1815 paroxysmal eruption of Tambora on the island of Sumbawa, 165 km to the East of Lombok (Stothers, 1984; Sigurdsson and Carey, 1989; 1992; Self et al., 1984; 2004; Sutawidjaja et al., 2006; Gertisser et al., 2012).

Fig. 25. Stop 9: Tsunami deposit with very poorly sorted stratified mixture of coral cobbles and volcaniclastic debris below the co-PDC fine ash deposit, AD 1815 eruption of Tambora, preserved on Lombok at STOP 9 (Luk coastal cliffs).

STOP 10: RIN-1373 (Sidutan river)

Elevation: 30 m	Distance to source: 26 km
Lat : S8°16‘51.4’’	Long : E116°13’38.1’’

From STOP 9 drive back to the main road in Montongpal and turn left towards the East in the direction of Kayangan, and Senaru further. Drive 1.7 km until you reach the small village on Sidutan on

the coast where there is a nice beach with palm trees. Park just after the main bridge, over the Sidutan River. Walk down to the Sidutan River and walk 500 m up the river (towards the SE) for about 10 minutes until you reach the 2nd large meander in the river with well-exposed ca. 30 m cliffs.

This is a very nice active quarry that exposes at least 20 m of the main stratigraphic sequence of the AD1257 eruption and the best section to the North of the caldera (**Fig. 26**). Overall, the units that are present in Stop 10 show similar sedimentological characteristics as in Stop 1 and 2 and 3. In addition to the thick non-welded pumiceous PDCs, the phreatoplinian blue gray fine ash unit rich in accretionary lapilli is particular prominent at this location with numerous layers including some intercalated distal dilute turbulent PDC layers. From base to top we observe:

- Phreatic vent opening phase: dark black (organic rich) massive, compact, fine-grained ash fall unit Ph-AF, 2-3 cm thick but variable.

- Ultraplinian phase UP1: very vesicular white pumice fall unit UP1-PF, 25 cm thick, reversely graded, rich in accidental clasts, very poorly sorted, massive, weakly stratified, coarse, fines poor. Indurated due to stream flow. Deposited on relatively flat ground (colluvium, old pumice fallout). Better sorted in the middle of the unit.

- Phreatoplinian phase PP, gray pumice fall unit PP-PF1, 4 cm, normally (?) graded, poorly but better sorted than PP-PF2, rich in accidental clasts, massive, loose, fines poor.

- Phreatoplinian phase PP, unit is 8.5 cm thick and consists of five layers: 1) PP-TPDC1: a 0.5-0.8 cm thick, rusty colored finely laminated fine ash layer, indurated, rich in accidental clasts; we interpret PP-TPDC1 as having been emplaced by distal dilute pyroclastic density currents (surges) associated with the phreatoplinian phase; 2) PP-ALF1: a 13 cm thick layer that is compact, blue gray (pyrite ?) fine ashfall layer rich in accretionary lapilli 3-6 mm in diameter, oxidized large pumice clasts; 3) PP-TPDC2: a 1.5 cm thick layer with compact indurated fine ash and wavy laminations, we interpret Ca as having been emplaced by distal dilute pyroclastic density currents (surges); 4) PP-TPDC3: a 4 cm thick layer of compact, blue gray (pyrite ?) fine ash layer rich in

accretionary lapilli 3-6 mm in diameter that shows wavy laminations and is erosive in the underlying layer; we interpret PP-TPDC3 as having been emplaced by distal dilute pyroclastic density currents (surges); 5) PP-TPDC4: a 8 cm thick orange-rusty and pinkish fine ash layer thinly laminated and with cross-stratifications, and containing altered accretionary lapilli; we interpret PP-TPDC4 as having been emplaced by distal dilute pyroclastic density currents (surges).

- Phreatoplinian phase PP, gray pumice fall unit PP-PF2, 3.5 cm thick laterally continuous constant thickness, reversely graded, poorly sorted, dark clast-rich, coarser than PP-PF1, fines poor, massive.

- Ultraplinian phase UP2, whitish gray pumice fall unit UP2-PF1, 5.5 cm thick, coarser than B1, better sorted, less rich in accidental clasts, massive, eroded by unit above.

- Ultraplinian phase UP2, pinkish compact massive fine ash unit UP2-TPDC with large subrounded vesicular pumice (2.5 cm), rich in large accidental clasts, vesicular matrix, laterally discontinous and erosive into unit UP2-PF1; we interpret UP2-TPDC as having been emplaced by distal dilute pyroclastic density currents (surges) associated with column collapse of the UP2 phase at the time of deposition of unit UP2-PF1.

- Ultraplinian phase UP2, fine-grained lenses, 2-3 cm thick, of pumice fallout unit UP2-PF2 (?), rich in accidental clasts, eroded by overlying unit UP2-PDC.

- Ultraplinian phase UP2, massive, compact, thinly laminated, pinkish, fine ash unit UP2-VTPDC1 that contains rounded pumice clasts (up to 2 cm), typical pinch and swell bedding, and is erosive into units UP2-PF2, UP2-TPDC, and UP1-PF; we interpret UP2-VTPDC1 as having been emplaced by distal dilute pyroclastic density currents (surges) associated with column collapse of the UP2 phase at the time of deposition of unit UP2-PF3.

- Ultraplinian phase UP2, Lenses 2-3 cm thick of pumice (2-3 cm in diameter) fallout unit UP2-PF3 (?), rich in accidental clasts, contain charcoals, eroded by the overlying unit UP2-VTPDC2.

- Ultraplinian phase UP2: the base of the lowermost PDC flow unit is an indurated, 28 cm thick unit (UP2-VTPDC2) that contains locally some lenses 6-12 cm thick of large rounded pumices (>7 cm in size) that are imbricated in the direction of flow, the unit is rich in accidental clasts, very well-sorted, fines poor, clast-supported with clasts elongated in the direction of flow. This unit has eroded rip-up clasts into the underlying pumice fallout unit UP2-PF3. This basal unit UP2-VTPDC2 is interpreted as having been deposited from a more dilute stratified high-energy current (ground layer).

- Ultraplinian phase UP2, sequence of several flow units UP2-PDCs of valley-ponding pumice-rich and ash-rich non-welded pyroclastic density current deposits (PDCs) reaching 20 m in thickness. The uppermost 2 units are more pinkish.
  From the Sidutan village, drive on the main road towards the NE for about 25 km to Anyar, then follow the main road that climbs North up to Bayam for about 3.7 km. Just before Bayam turn right and drive up for about 4 km to Senaru on a smaller paved road.
  Arrive at Senaru (601 m; 8°17'53.40"S; 116°24'30.54"E) around 18:00. Early diner and briefing for the hike to the caldera rim.

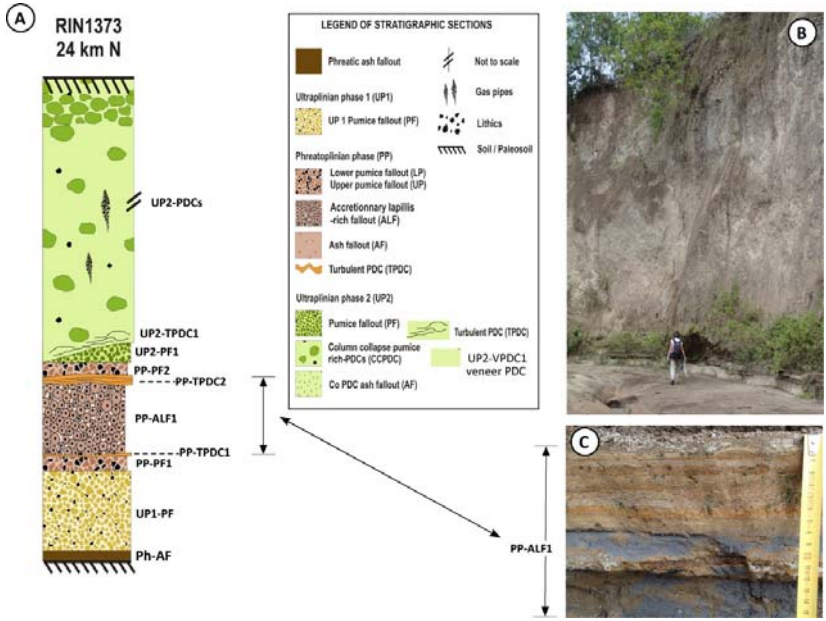

Fig. 26. Stop 10: A: Stratigraphic log of the sequence of deposits seen in the 15 m cliff of the Sidutan river. B: view of the oucrop with geologist for scale with feet at the level of the A UP1 pumice fallout unit. c: detail of the phretoplinian C unit with blue gray characteristic compact fine ash unit rich in larger accretionary lapilli and overlying distal dilute turbulent PDC layers (Vidal et al., 2013; in prep.).

DAY 4

We will wake up at 6:00 and start to climb up at 7:30 for the long 10.5 km to the Plawangan camp site (2641 m; 8°22'59.28"S; 116°24'4.44"E) on the Senaru northern caldera rim. The hike will take ca. 7-8 hours ascent including lunch stops and resting stops for a net elevation gain of 2000 m (**Fig. 27; 28**).

There are several resting stops with shelters named POS1 (915 m), POS EXTRA (1165), POS2 (1500 m), POS3 (2000 m), and the camp site (Plawangan / Senaru crater rim) on the north rim (2641 m) which is at tha start of the trail going down the N rim of the caldera to the lake shore (2000 m) (**Fig. 27; 28**).

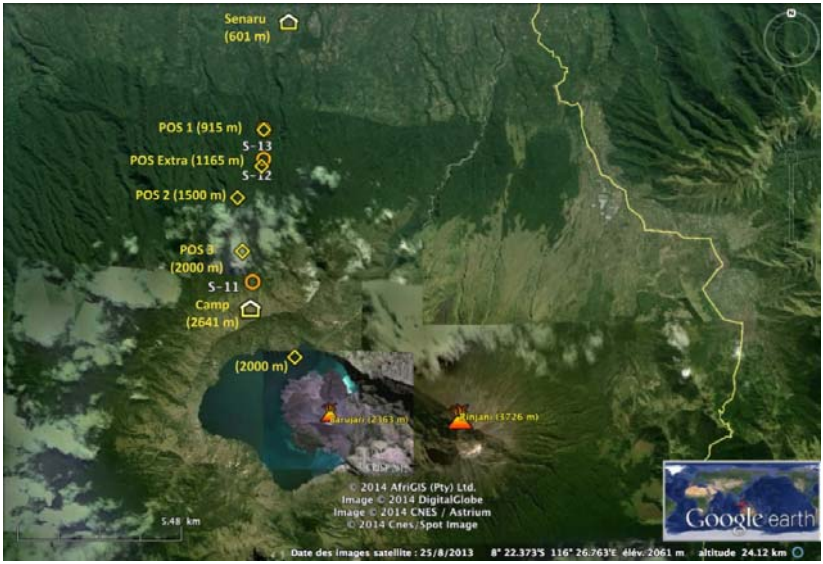

Fig. 27. Stops 11-13: Satellite image of the Anak Segara crater, Rinjani volcano, and the northern flanks of the Samalas-Rinjani volcanic complex with stops and landmarks related to the hike to the Senaru northern rim of the caldera. Modified from Google Earth, satellite imagery provided to Google Earth by providers (see image for credits).

GIVEN TIME AND LOGISTICAL CONSTRAINTS AS WELL AS THE ADDITIONAL 4 HOURS (DOWN AND UP) ON A STRENUOUS DIFFICULT PATH, WE WILL NOT GO DOWN TO THE LAKE SHORE INSIDE THE CALDERA.

On Day 4 we will make only one official stop (S-11) going up above POS3. It is best to do most stops going down and thus climb "straight" on Day 4 without losing time for additional geology stops to try to get a sunset view at the caldera rim and allow time for variable climbing times. We can make additional stops around the camping area as we wish.

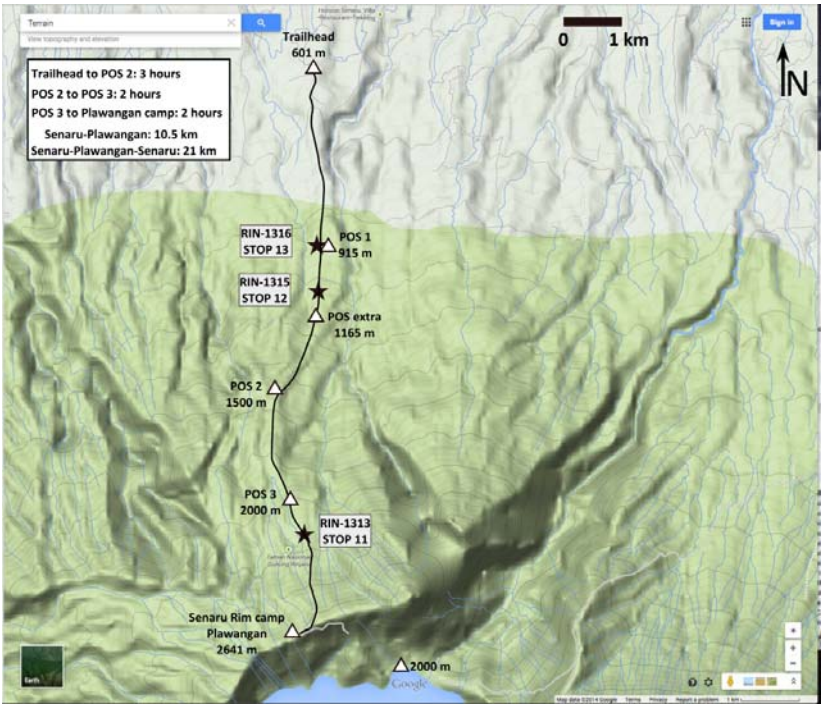

Fig. 28. Stops 11-13: Shaded relief map of the northern flank of the Samalas-Rinjani volcanic complex with stops, landmarks and information related to the hike to the Senaru northern rim of the caldera. Modified from Google Maps.

Most of the AD1257 sequence of proximal fallout units has been eroded on the flanks of the Samalas volcano by turbulent dilute PDCs associated with the PP and UP2 phases of the AD1257 eruption. The units seen along the trail are essentially those of pre-AD1257 explosive eruptions including thick and extensive high-alumina basalt scoria fallout units (Vidal et al., 2013; 2014; in prep.) and older stratified yellowish pumice fallout and intercalated dilute PDC units that we will discuss at STOP 11 and on Day 5 at STOPS 12 and 13.

Above POS3 we will walk on massive pre-AD1257 lava flows that belong to Samalas volcano, before we see near the camp site

patches of the proximal welded facies of a pumice explosive breccia from the AD1257 eruption.

STOP 11: RIN-1313 (above POS 3)

Elevation: 2138 m	Distance to source: 4 km
Lat : S8°22‘22.4’’	Long : E116°24’04.4’’

About 30 minutes above POS 3, at the start of the steeper slope and more scattered vegetation we reach STOP 11 along the trail. We observe here pre-AD1257 scoria deposits of unknown but Holocene age. From base to top we see:

- Holocene plinian Holocene phase, reversely graded, poorly sorted, coarse (3-4 cm clasts) partly altered yellow pumice fallout unit, > 35 thick, rich in accidental clasts, and containing two types of juvenile vesicular clasts, dominant yellowish well vesiculated pumice and subordinant gray very finely vesicular to weakly vesicular denser pumice with angular polygonally-shaped faces. We have seen periodically this unit along the path and especially a bit below STOP 11 at a non-visited outcrop (RIN-13-14 at about 2040 m of elevation just above POS 3) where it outcrops without the scoria above, thus presumably eroded ? The challenge in this part of the trail is to unravel the stratigraphy given that units appear and disappear in a small spatial zone given the very steep slope and the effects of intense surface remobilization and erosion of several thousands of years.

- Holocene massive fine ash fallout unit 17cm thick.

- Holocene violent strombolian ? – plinian ? phase, loose, massive to weakly stratified, well to very poorly sorted thick scoria fallout unit forming 5 distinct layers (57 cm at the base, 49 cm, 65 cm, 8 cm, and 100 cm at the top, 0.65, 0.49, 0.57, and 0.57 cm in thickness) of variable thickness given their deposition on a very steep slope. The units show varying average grain size from coarse sand to coarse lapilli and variable sorting. The coarsest and thickest upper-most unit is the most stratified with trains of coarse scoria lapilli aligned along the plane of steepest slope. Each unit typically ends with an upper reddish oxidized 5-6 cm thick zone. The distribution of this deposit needs to be assessed in detail but the widespread dispersal,

thickness at distances of 4 to 8 km (>2 m at 1860 m of elevation) and the moderate sorting and the lack of a very pronounced bedding suggest that eruption flux was high and relatively sustained and that the volume emitted could be significant. The units are likely to have been produced by very intense sustained strombolian activity and perhaps even plinian activity. This is particularly interesting given the high-alumina basalt composition (Vidal et al., 2013; 2014; in prep.) of these products from the Samalas-Rinjani volcanic complex. Nasution et al. (2004; 2010) have obtained ^{14}C dates of 11940 ± 40 y. B.P., 11980 ± 40 years B.P., and 5990 ± 50 years B.P. for three scoria fall units on the northern flank of Rinjani which are likely these units. We make the hypothesis that the sequence seen here is likely the youngest one dated at 5990± 50 years B.P. by Nasution et al. (2004).

We will camp overnight on top of the caldera rim (2641 m) overlooking the majestic Segara Anak Lake (2000 m) and Barujari cone (2363 m), and dominated by the Rinjani edifice (3726 m).
The northern rim of the caldera is covered by proximal facies of the AD 1257 pumice pyroclastic flows with locally welded facies including very coarse proximal pumice breccia units. The uppermost mantling units consists of ash and scoria fallout material from historical eruptions of Barujari since AD 1847 (CVGHM, Global Volcanism Network).

The Segara Anak caldera contains the breathtaking Segara Anak lake, "Child of the Sea", a 230-m-deep turquoise blue lake (**Fig. 29**) whose shores lie at 2000 m above sea level. It covers an area of 11km^2 and its volume was (before the 2009 eruption) estimated at 1.02 km^3 (Barbier, 2010). Segara Anak is thought to be the home of the Gods for many local Sasak and Balinese people who organize a spiritual ceremony of offerings to its magnificent blue water believed to purify the soul and heal the body. The lake is neutral (pH: 7-8) and its chemistry dominated by chlorides and sulfates with a relatively high TDS (Total Dissolved Solids: 2640 mg/l). This unusual TDS as well as the lake surface temperatures (20-22°C) well above ambient temperatures (14-15°C) for this altitude, reflect a strong input of hydrothermal fluids with an estimated temperature of 270°C. Hence, Segara Anak has one of the largest volcanic lake thermal anomaly (1700 MW) and $C0_2$ emission flux of volcanic origin in the world

(Barbier, 2010). Numerous hot springs are located along the shore at the foot of Gunung Baru volcanic cone. Bathymetric profiles show also several areas with column of gas bubbles escaping from the lake's floor and indicating a significant discharge of CO2 gas into the lake (Barbier, 2010).

The caldera has been partly filled by the continuing growth of the post-caldera cone Barujari whose known historical eruptions date back to 1847 (**Fig. 11**). They consist of moderate explosive activity and occasional lava flows that have entered Segara Anak lake. The last eruption of Barujari occured in 2009-2010 (**Fig. 11)**. The active caldera complex of Rinjani is monitored permanently by an Observatory (**Fig. 10A**) operated by PVMBG (CVGHM). Lahar hazard is elevated at Rinjani given the size of the caldera lake, volcanic activity, potential landslide into the lake from the steep caldera internal walls, the limited height of the lava damming the lake outlet into the Lokok Putih river, as well as the production during explosive eruptions of copious amounts of ash coupled with the intense precipitation in the rainy season. In the context of continuing eruption, on 3 November 1996 a small cold lahar in the Kokok Jenggak River killed 30 people collecting drinking water in the river (CVGHM, 1996). The caldera has a complex, polyphase morphology, it is 8.2 km in the East-West axis from the edge of the Rinjani edifice collapse scar to the caldera rim and 5.42 km in the North-South direction (**Fig. 13B**). If we excluded the U-shaped depression formed by the Rinjani edifice collapse into the AD1257 caldera which probably occurred shortly after the eruption (Takada et al., 2003; Nasution et al., 2004; Lavigne et al., 2013), the actual caldera is 5.4 x 5.36 km and roughly circular with scalloped edges. The caldera depth is about 500-700 m on average except on the Rinjani side where the drop off from Rinjani's summit above the lake is 1726 m ! We can observe the internal structure (dikes, lava flows) of the different volcanic edifices that form the very large Samalas-Rinjani volcanic complex whose surface area is roughly 25 x 30 km if we include some of its longuest known lava flows. The complex morphology of the caldera is likely the result of several caldera formation stages with the most recent dated at AD 1257 as well as the influence of tectonic structures. The caldera rim is dissected by several major and deep (ca. 600 m) U to V-shaped valleys whose morphology likely reflects the interplay of several major catastrophic

processes such as caldera collapse and edifice collapse, structural tectonic control, erosion by passage of large-volume caldera collapse pyroclastic flows, catastrophic flood release from the caldera lake , landsliding, and intense erosion.

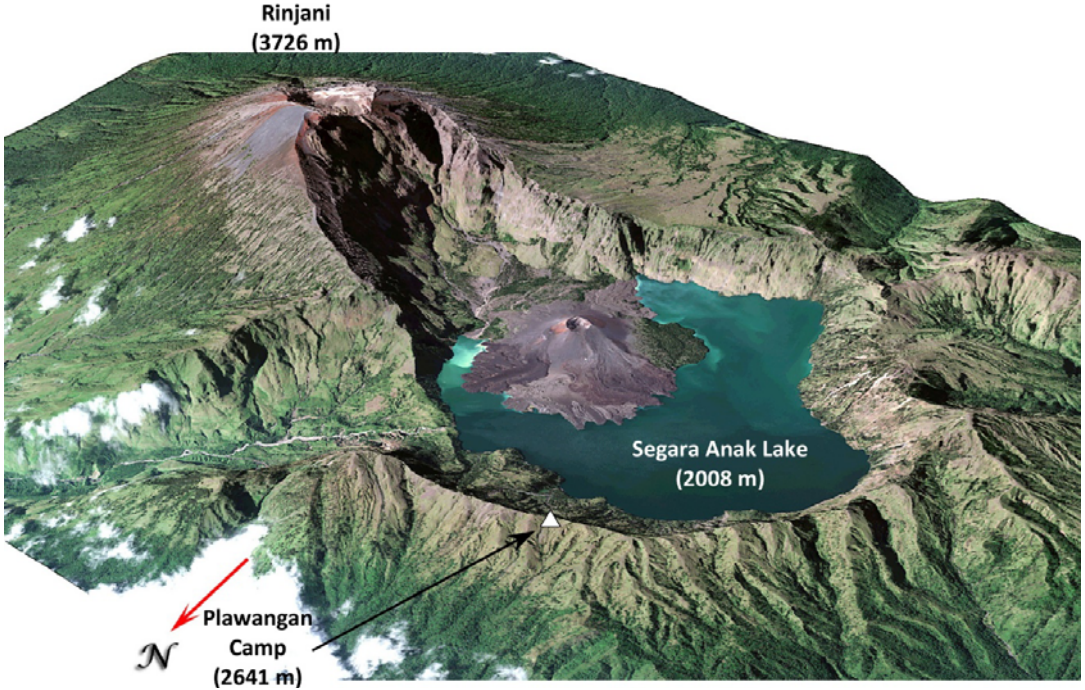

Fig. 29. Satellite image of Segara Anak caldera (26 June 2012) draped on shaded-relief view (traingle is the Plawangan camp site). Geoeye-1 Satellite Image © Centre for Remote Imaging, Sensing and Processing, National University of Singapore (2012), terrain views rendered using SRTM 3 data from NASA.

Fig. 30. Panoramic view of magestic Anak Segara caldera lake (2000 m elevation) from the Senaru north caldera rim campsite at Plawangan (2641), looking South, with Rinjani (3726 m) summit and crater to the left and the active Barujari cone (2363 m) in the foreground with its recent lava flows emitted since 1944 and last in 2009. Photo J-C Komorowski

DAY 5

We will wake up at 6:00 and start to descend up at 7:30 for the long 10.5 km (ca. 7-8 hours) trail to Senaru (601 m). We will make 2 short stops along the way, S-12, and S-13 going down to Senaru for the return distance of 10.5 km.

STOP 12: RIN-1315 (below POS extra)

Elevation: ca 1100 m Distance to source: 8 km
Lat : S8°20‘13.8’’ Long : E116°24’07.9’’

After about 5-6 hours of walking down from the summit we arrive at STOP 12, about 20 minutes below the POS Extra rest stop. Here we can see the stratigraphic relationship between one the recent black scoria fallout units that underlies an upper yellow plinian pumice fallout unit that we have seen repeatedly over the path including at the unvisited outcrop of RIN-13-14 at an elevation of 2040. At STOP 12 we see from the base to the top:

- Holocene violent strombolian ? – plinian ? phase, loose, non graded, massive, very well sorted coarse ash to fine lapilli scoria fallout unit > 1 m thick. This is probably the oldest of the 3 scoria fallout units dated by Nasution et al. (2004; 2010) at 11940 ± 40 y. B.P., and 11980 ± 40 years B.P. because it occurs below the yellow pumice which we saw at STOP 12 to be at the base of a thick sequence of the youngest scoria fallout units. The reconstruction of the Holocene eruptive stratigraphy is presently being refined (e.g. Vidal et al., 2014; Furukawa et al., 2014).

- Holocene dark grey thinly laminated fine ash fallout unit 7-8cm thick.

- Holocene plinian Holocene phase, non graded, poorly sorted, coarse (3-4 cm clasts) partly altered yellow pumice fallout unit, > 35 thick, rich in accidental clasts, and containing two types of juvenile vesicular clasts, dominant yellowish well vesiculated pumice and subordinant gray very finely vesicular to weakly vesicular denser pumice with angular polygonally-shaped faces. We have seen periodically this unit along the path and especially a bit below STOP 11 at a non-visited outcrop (RIN-13-14 at about 2040 m of elevation

just above POS 3) where it outcrops without the scoria above, thus presumably eroded ?

STOP 13: RIN-1316 (at POS 1)

Elevation: 915 m Distance to source: 10 km
Lat : S8°19‘42.08’’ Long : E116°24’07.1’’

After another hour of walking down from the summit we arrive at STOP 13, the last stop of the excursion at the POS 1 resting area.
Here we can see an additional sequence of alternating pumice fallout units and intercalated ashfall and turbulent dilute PDC units of the Holocene activity of Samalas-Rinjani volcanic complex. Given the limited exposure, it remains difficult to fit this sequence in the Holocene stratigraphy with respect to the scoria fallout units that we have seen coming down on the trail since at STOP 11 and that were described briefly by Nasution et al. (2004; 2010) who dated them at 11940 ± 40 y. B.P., and 11980 ± 40 years B.P., and 5990 ± 50 years B.P. This complex sequence here resembles the sequence described by Nasution et al. (2004) as the Propok Pumice that was erupted from another volcanic center, Propok volcano located east of Samalas-Rinjani (Nasution et al., 2004; 2010). This remains to be reconstructed with further detail.

Walk the last hour to the Rinjani National Park entrance.

After the end of the hike and the return to Senaru around 15:00, we will drive back straight to Senggigi hotel (aprox. 3h). We will stop at around 18:00, time-allowing, at a road overlook just before arriving to Senggigi, to enjoy a nice sunset over Agung. We will have a final diner at the hotel around 20:00.

DAY 6

After the breakfast the excursion will end and participants can leave to their next destination.

References

Barbier, B., 2010. Bilan thermique et caractérisation géochimique de l'activité hydrothermale du volcan Rinjani (Lombok, Indonésie), Université Libre de Bruxelles Faculté des Science, Département des Sciences de la Terre et de l'Environnement, Laboratoire de Géochimie et Minéralogie Appliquée, Thèse de Doctorat, 1-265 pp. http://theses.ulb.ac.be/ETD-db/collection/available/ULBetd-04282010-165329/unrestricted/totaldelmelle2.pdf

Bemmelen, R.W van, 1949 The Geology of Indonesia vol.IA, General Geology, Martinus Nyijjhoff The Hague.

Bonadonna C., Costa A. (2013). Plume height, volume, and classification of explosive volcanic eruptions based on the Weibull function, Bulletin of Volcanology 75, 742-762.

Bull, I.D., Knicker, H., Poirier, N., Porter, H.C., Scott, A.C., Sparks, R.S.J., Richard, P., 2008. Evershed, biomolecular characteristics of an extensive tar layer generated during eruption of the Soufrière Hills volcano, Montserrat, West Indies. Organic Geochemistry 39, 1372–1383.

Connell B, et al. (2012) A Bioarchaeological Study of Medieval Burials on the Site of St Mary Spital: Excavations at Spitalfields Market, London E1, 1991–2007 (Museum of London Archaeology, Monograph Series 60, London).

Delisle L, Jourdain CMG, Wailly DEN eds (1877) Chronique Anonyme des Rois de France Finissant en 1286. Tome 21, Recueil des historiens des Gaules et de la France, (Victor Palmé, Paris) pp. 81–102.

Druitt, T.H., Calder, E.S., Cole, P.D., Hoblitt, R.P., Loughlin, S.C., Norton, G.E., Ritchie, L.J., Sparks, R.S., Voight, B., 2002. Small-volume, highly mobile pyroclastic flows formed by rapid sedimentation from pyroclastic surges at Soufrière Hills volcano, Montserrat: an important volcanic hazard. In: Druitt, T.H., Kokelaar, B.P. (Eds.), The eruption of Soufrière Hills volcano,

Montserrat, from 1995 to 1999: Mem Geol Soc London, 21, pp. 263–280.

Foden, J.D., 1983. The petrology of the calc-alkaline lavas of Rinjani volcano, East Sunda Arc: a model for island arc petrogenesis. Journal of Petrology Vol. 24, Part 1 pp 98-130.

Furukawa, R., Takada, A., Nasution, A., 2005. Eruptive sequence of 13th century caldera formation at RInjani volcano, Lombok, Indonesia. Coordinating Committee for Geoscience Programmes in East and SOutheast Asia (CCOP), The Second Field Workshop for Volcanic Hazard Mitigation, Merapi, Kelut Volcanoes, Indonesia, September 5-11, 2005, abstract.

Furukawa, R., Takada, A., Nasution, A. 2014. Stratigraphy and caldera formation of Rinjani volcano, Lombok, Indonesia. Cities on Volcanoes COV8, "Living in harmony with volcano, bridging the will of nature to society", International Association of Volcanology and Chemistry of the Earth's Interior (IAVCEI), Yogyakarta, Indonesia, 9-13 September 2014, abstract, poster.

Gao C., Oman L., Robock A., Stenchikov L., (2007). Atmospheric volcanic loading derived from bipolar ice cores: Accounting for the spatial distribution of volcanic deposition. Journal of Geophysical Research 12, D09109, doi:101029/2006JD007461.

Gao, C. C., Robock, A. & Ammann, C., 2008. Volcanic forcing of climate over the past 1,500 years: An improved ice core-based index for climate models. J. Geophys. Res. **113,** D23111.

Gertisser, R., Self, S., Thomas, L.E., Handley, H.K., Van Calsteren, P., Wolf, J.A., 2012. Processes and timescales of magma genesis and differentiation leading to the great Tambora eruption in 1815. Jour. Petrology, Vol. 53, No. 2, 271-297, doi:10.1093/petrology/egr062.

Giles JA ed and trans (1854) Matthew Paris's English History. From the Year 1235 to 1273 Vol. 3 (Henry G. Bohn, London) pp. 256–257.

Global Volcanism Program, Natural History Museum Smithsonian Institution, http://www.volcano.si.edu, accessed 5 August 2014.

Kandlbauer, J., Carey, S.N., Sparks, R.S.J., 2013. The 1815 Tambora ash fall: implications for transport and deposition of distal ash on land and in the deep sea. Bull Volcanol (2013) 75:708, 11 pages, DOI 10.1007/s00445-013-0708-3.

Kurbatov A.V. et al., (2006). A 12,000 year record of explosive volcanism in the Siple Dome Ice Core, West Antarctica. Journal of Geophysical Research 111, D12307.

Kusumadinata, K., 1969 Sejumlah Data Mengenai Danau Kawah Segara Anak Di Pegunungan Rinjani, Lombok. Direktorat Vulkanologi.

Kusumadinata, K., 1979 Data Dasar Gunungapi Indonesia. Catalogue Of References On Indonesian Volcanoes With Eruptions In Historical Time, p424-438, Direktorat Vulkanologi.

Kusnadi, I., Tulus, C. Sulaeman, M.E. Ilyas, Kusma, Rahmanto, Mutaharlin and L. Zulkarnain, 1994. Laporan Pengamatan Gempa Dan Pemeriksaan Kawah G. Rinjani, Juni—September 1994. Direktorat Vulkanologi.

Kusnadi. I., & A. Gunalan, 1995 Laporan Pengamatan/ Pengawasan G. Rinjani, September 1995. Direktorat VulkanologiHadisantono, R.D., Heriwaseso, A., Pujowarsito, Riyadi, dan Dahlan, A. 2008. Peta kawasan rawan bencana gunungapi Rinjani, provinsi Nusa Tenggara Barat. Pusat Vulkanologi dan Mitigasi Bencana Geologi.

Kusnadi, I & Ilyas, M.E., 1997 Laporan Pengamatan G. Rinjani, Agustus 1997. Direktorat Vulkanologi.

Lavigne F., Guillet S., Khodri M., Degeai J.-P., Robert V., Komorowski J.-C., Vidal C., Robin A.-K., Kuzucuoglu C., Wassmer P., Sri Hadmoko D., Lahitte P., Virmoux C., Brunstein D., Grancher D., (2012). The 1258 Mystery eruption: Environmental Effects, Time of Occurrence and Volcanic Source, AGU Chapman Conference on Volcanism and the Atmosphere,

Selfoss, Iceland, 10 – 15 June 2012, abstract p. 44; http://www.agu.org/meetings/chapman/2012/bcall/.

Lavigne, F., Degeai, J-P., Komorowski J-C**,** Guillet, S., Robert, V., Lahitte, P., Oppenheimer, C., Stoffel, M., Vidal, C., Pratomo, I., Wassmer, P., Hajdas, I., Sri Hadmoko, D., de Bélizal, E. (2013). Source of the great A.D. 1257 mystery eruption unveiled: Samalas volcano, Rinjani volcanic complex, Indonesia. *Proceedings of the National Academy of Sciences, USA* (PNAS), www.pnas.org/cgi/doi/10.1073/pnas.13075201100.

Lavigne, F., Komorowski, J-C., Degeai, J-P., Robert, V., Hadmoko, D. Sri, Pratomo, I., Vidal, C., de Belizal, E., Lahitte, P., 2014. Local legend or historical source? The Babad Lombok as a testimony of the AD 1257 eruption of Mount Samalas/Rinjani, Lombok Island, Indonesia. Cities on Volcanoes COV8, "Living in harmony with volcano, bridging the will of nature to society", International Association of Volcanology and Chemistry of the Earth's Interior (IAVCEI), Yogyakarta, Indonesia, 9-13 September 2014, oral.

Luard HR ed (1872–1873) Matthaei Parisiensis monachi sancti Albani Chronica Majora Rerum britannicarum medii aevi scriptores Vol. 5 (London) pp. 661–662.

Miller, C.F. & Wark, D.A. (2008). Supervolcanoes and their explosive super-eruptions. Elements 4/1, 11-16.

Miller G.H. et al., (2012). Abrupt onset of the Little Ice Age triggered by volcanism and sustained by sea-ice/ocean feedbacks. Geophysical Research Letters 39, L02708 10.

Nasution A, Takada A, Rosgandika M. (2004) The volcanic activity of Rinjani, Lombok Island, Indonesia, during the last the thousand years, viewed from ^{14}C datings. Convention Bandung 2004, The 33rd annual Convention & Exhibiution, Indonesian Association of Geologist, Horizon Hotel, 29-30 Nov. 2004, Bandung, extended abstract, 8 pp.

Nasution A, Takada A, Udibowo, Widarto D, Hutasoit L (2010) Rinjani and Propok volcanics as a heat sources of geothermal

prospects fron eastern Lombok, Indonesia. Jurnal Geoaplika 5(1):1–9.

Oppenheimer C (2003) Ice core and palaeoclimatic evidence for the timing and nature of the great mid-13th century volcanic eruption. Int J Climatol 23(4):417–426.

Oppenheimer, C., Scaillet, B., Martin, R.S., 2011. Sulfur Degassing From Volcanoes: Source Conditions, Surveillance, Plume Chemistry and Earth System Impacts, Reviews in Mineralogy & Geochemistry, Vol. 73 pp. 363-421.

Palais JM, Germani MS, Zielinski GA (1992) Interhemispheric transport of volcanic ash from a 1259 A.D. volcanic eruption to the Greenland and Antarctic ice sheets. Geo- phys Res Lett 19(8):801–804.

Rodysill, J.R., Russell, J.M., Bijaksana, S., Brown, E.T., Safiuddin, L.O., Eggermont, H., 2012. A paleolimnological record of rainfall and drought from East Java, Indonesia during the last 1,400 years. J. Paleolimnol. 47, 125-139.

Santosa, I. & I. Sinulingga, 1994 Laporan Penyelidikan Petrokimia Gunungapi Rinjani. Direktorat Vulkanologi.

Schneider D. P. Ammann C. M., Otto-Bliesner B. L., Kaufman D. S. (2009). Climate response to large, high-latitude and low-latitude volcanic eruptions in the Community Climate System model. Journal of Geophysical Research 114, D15101.

Scott, A.C., Sparks, R.S.J., Bull, I.D., Knicker, H., Evershed, R.P., 2008. Temperature proxy data and their significance for the understanding of pyroclastic density currents. Geology, 36-2: 143-146.

Self, S., Rampino, M. R., Newton, M. S. & Wolff, J. A. (1984). Volcanological study of the great Tambora eruption of 1815. Geology 12, 659-663.

Self, S., Gertisser, R., Thordarson, T., Rampino, M. R. & Wolff, J. A. (2004). Magma volume, volatile emissions, and stratospheric

aerosols from the 1815 eruption of Tambora. Geophysical Research Letters 31, L20608, doi:10.1029/2004GL020925.

Sigl, M, McConnell, J.R., Toohey, M., Curran, M., Das, S.B., Edwards, R., Isaksson, E., Kawamura, K., Kipfstuhl, S., Krüger, K., Layman, L., Maselli, O.J., Motizuki, Y., Motoyama, H., Pasteris, D.R., Severi, M., 2014. Insights from Antarctica on volcanic forcing during the Common Era, Nature Climate Change, PUBLISHED ONLINE: 6 JULY 2014 | DOI: 10.1038/NCLIMATE2293; Vol. 4, August 2014, 693-697.

Sigurdsson, H. & Carey, S. (1989). Plinian and co-ignimbrite tephra fall from the 1815 eruption of Tambora volcano. Bulletin of Volcanology 51, 243-270.

Sigurdsson, H. & Carey, S. (1992). The eruption of Tambora in 1815: environmental effects and eruption dynamics. In: Harrington, C. R. (ed.) The Year without a Summer?: World Climate in 1816. Ottawa: Canadian Museum of Nature, pp. 16-45.

Sparks, R.S.J., Barclay, J., Calder, E.S., Herd, R.A., Komorowski, J.-C., Luckett, R., Norton, G.E., Ritchie, L.J., Voight, B., Woods, A.W., 2002. Generation of a debris avalanche and violent pyroclastic density current on 26 December (Boxing Day) 1997 at Soufrière Hills volcano, Montserrat. In: Druitt, T.H., Kokelaar, B.P. (Eds.), Geological Society, London, Memoirs 21, 409–434.

Stothers, R. B. (1984). The great Tambora eruption in 1815 and its aftermath. Science 224, 1191-1198.

Stothers RB (2000) Climatic and demographic consequences of the massive eruption of 1258. Clim Change 45(2):361–374.

Sulaeman and Muarif, 1998 Kegempaan G. Rinjani Periode 1995—1998. Direktorat Vulkanologi.

Sundhoro, H., 1992 The Sembalun Geothermal Field, East Lombok, West Nus Tenggara, Indonesia. Kumpulan Karya Ilmiah Hasil Penyelidikan Gunungapi dan Panasbumi p 39--59. Direktorat Vulkanologi.

Sutawidjaja I.S., Sigurdsson, H., Abrams, L., 2006. Characterization of volcanic deposits and geoarchaeological studies from the 1815 eruption of Tambora volcano. Jurnal Geologi Inodnesia, Vol. 1, No. 1, Maret 2006, 49-57.

Takada A, Nasution A, Rosgandika M. (2003) Eruptive history during the last 10ky for the caldera-forming eruption of Rinjani volcano. Japan Geoscience Union meeeting, 2003, www2.jpgu.org/meeting/2003/.

The Columbia Encyclopedia, 6th ed.. 2013. “flagellants.", Retrieved August 05, 2014 from Encyclopedia.com: http://www.encyclopedia.com/doc/1E1-flagella.html

Vidal, C. M., Metrich, N., Komorowski J.-C, Pratomo, I., Lavigne, F., Surono , 2013, Insights into the Magmatic Processes Leading to the Holocene Caldera Eruption of Rinjani, Indonesia. Goldschmidt 2013 International Conference, 25-30 Augut 2013, Florence, Italy, Mineralogical Magazine, 77(5), 2413, oral.

Vidal, C., Komorowski, J-C., Métrich, N., Pratomo, I., Prambada, O., Kartadinata, N., Lavigne, F., Fontijn, K., Rodysill, J., Michel, A., 2014. Eruptive dynamics of the A.D. 1257 ultraplinian eruption of Rinjani Samalas (Lombok, Indonesia), Cities on Volcanoes COV8, "Living in harmony with volcano, bridging the will of nature to society", International Association of Volcanology and Chemistry of the Earth's Interior (IAVCEI), Yogyakarta, Indonesia, 9-13 September 2014, oral.

Vidal, C., Komorowski, J-C., Métrich, N., Pratomo, I., Prambada, O., Kartadinata, N., Lavigne, F., Fontijn, K., Rodysill, J., Michel, A. Eruptive dynamics of the recently discovered ultraplinian A.D. 1257 eruption of Rinjani Samalas (Lombok, Indonesia), Bull Volcanol, in prep.

Voight, B., Komorowski, J.-C., Norton, G., Belousov, A., Belousova, M., Boudon, G., Francis, P., Franz, W., Sparks, S., Young, S., 2002. The 1997 Boxing Day sector collapse and debris avalanche, Soufrière Hills Volcano, Montserrat, B.W.I. In: Druitt, T., Kokelaar, B.P. (Eds.), The Eruption of Soufrière Hills volcano,

Montserrat, from 1995–1999: Mem Geol Soc Lond, 21, pp. 363–407.

Wacana L (1979) Babad Lombok. (Departemen Pendidikan dan Kebudayaan, Proyek Penerbitan Buku Bacaan dan Sastra Indonesia dan Daerah, Jakarta).

Zielinski, G.A. et al., Record of volcanism since 7000 B.C. from the GISP2 Greenland ice core and implications for the volcano-climate system. Science 264, 948 (1994).

Hendrasto, M., E. Kadarsetia, D. Mulyadi and A. Nasution Pemetaan Geologi Gunungapi Komplek Rinjani, Lombok, Nusa Tenggara Barat. Direktorat Vulkanologi.

Multi Media Production, 1999 Informasi Proyek Batu Hijau, Newmont Nusa Tenggara.

Priatna and A. Saefudin, 1994 Laporan Penyelidikan Kimia Gas Dan Air, G. Rinjani, Nusa Tenggara Barat. Direktorat Vulkanologi